TUM School of Life Sciences

Novel fate-mapping system identifies replacement of resident cells during secondary infection

Madlaina von Hößlin

Vollständiger Abdruck der von der TUM School of Life Sciences der Technischen Universität München zur Erlangung des akademischen Grades einer Doktorin der Naturwissenschaften (Dr. rer. nat.) genehmigten Dissertation.

Vorsitzender: Prof. Dr. Harald Luksch

Prüfende der Dissertation:

1. Prof. Dr. Dietmar Zehn
2. Prof. Dr. Percy A. Knolle
3. Prof. David Masopust, Ph.D.

Die Dissertation wurde am 28.06.2021 bei der Technischen Universität München eingereicht und durch die TUM School of Life Sciences am 30.05.2022 angenommen.

Kurzfassung

Residente Gedächtnis $CD8^+$ T-Zellen (Trm) verbleiben nach einer Infektion im peripheren und lymphoiden Gewebe und bilden eine erste Verteidigungslinie gegen wiederkehrende Erreger. Ihre phänotypischen Eigenschaften und ihre Ortsgebundenheit sind gut untersucht, dennoch gibt es noch große Unklarheiten über ihre genaue Funktion, Kinetik und Beständigkeit während einer Reinfektion. Dies liegt im Besonderen daran, dass bislang keine Fate-Mapping Systeme zur Verfügung standen, die eine zuverlässige, eindeutige und langfristige Identifikation ermöglichen.

In dieser Arbeit wird daher erstmals das Verhalten und der spezifische funktionelle Beitrag von Trm während einer Reinfektion mit Hilfe eines neuen, hochspezifischen Trm-Fate-Mapping-Modells untersucht.

Das Fate-Mapping System ermöglicht die zuverlässige Markierung von Trm zu streng kontrollierten Zeitpunkten und eine Nachverfolgung über lange Zeiträume hinweg.

Während systemischer oder lokaler Restimulation zeigten $CD103^+$ Trm ein unerwartet geringes Reexpansionspotential und wurden durch neu gebildete $CD103^+$ Trm ausgetauscht. Es wurde nachgewiesen, dass sich $CD103^+$ Trm weder in der Peripherie noch in drainierenden Lymphknoten während der Reinfektion wieder finden, was ihre Ortsgebundenheit demonstrierte. Eine RNA-Sequenzierung zeigte, dass $CD103^+$ Trm früh während der Reinfektion von Inflammation reaktiviert werden können und über eine zusätzliche antigenspezifische Gensignatur verfügen, die die Balance zwischen Pathogenabwehr und Gewebeschutz leistet.

Dies führte zu der Schlussfolgerung, dass $CD103^+$ Trm den Host nicht durch ihre Reexpansion schützen, sondern in Geweben auf Antigen reagieren und übermäßige Gewebeschädigung verhindern.

Abstract

Resident memory $CD8^+$ T cells (Trm) remain in peripheral and lymphoid tissues after infection and form a first line of defense against recurrent pathogens. Their phenotypic properties and residence are well studied, yet there is still much uncertainty about their precise function, kinetics, and persistence during reinfection. This is since no fate-mapping systems have been available so far that allow reliable, unambiguous, and long-term identification.

This work therefore investigates for the first time the behavior and specific functional contribution of Trm during reinfection using a new, highly specific Trm fate-mapping model.

The fate-mapping system allows reliable labelling of Trm at tightly controlled time points and tracking over long periods of time.

During systemic or local restimulation, $CD103^+$ Trm showed an unexpectedly low reexpansion potential and were replaced by newly formed $CD103^+$ Trm. $CD103^+$ Trm were not found in the periphery or in draining lymph nodes during reinfection, which demonstrates their site-specificity.

RNA-sequencing revealed that $CD103^+$ Trm can be reactivated by inflammation early during reinfection and show an additional gene set in response to cognate restimulation, which balances pathogen elimination with tissue integrity.

This led to the conclusion, that $CD103^+$ Trm do not protect by reexpansion but act as sentinels that protect the host from pathogens and prevent excess tissue damage.

Contents

Chapter 1

Introduction

1.1 The protective immune system

The immune system is constantly defending the host from infections caused by pathogens like viruses or bacteria. In the process, pathogens are cleared, and protection mechanisms are installed against future reinfections. An improved understanding of the underlying mechanisms allows to support and induce these defense mechanisms for improved immediate and future protection.

The immune response uses versatile mechanisms to recognize pathogens and render them harmless. During the process, the immune response is tailored from a broad antigen unspecific reaction to a highly pathogen specific intervention. First the innate immune response acts fast and recognizes conserved foreign structures or signs of host damage rapidly and highly specific. Cells of the innate immune system can directly mediate defense mechanisms, like phagocytosis, and induce an inflammatory state of the infected tissue by producing pro-inflammatory cytokines (Chertov et al. 2000; Larsson et al. 1999; Carrero et al. 2004). If the infection cannot be eliminated by the innate immune response their action leads to an induction of the adaptive immune response and a containment of the pathogen at the site of infection (Germain 1994).

The adaptive immune response is induced in local lymphoid tissue, which leads to the activation of T cells and B cells. They have the unique ability to react to a great variety of pathogen derived antigens and form immunological memory. B cells produce antibodies, that are secreted to flag foreign agents as dangerous and thereby lead to neutralization of pathogens (Seidman and Leder 1978). T cells are divided into $CD4^+$ T cells and $CD8^+$ T cells and recognize intracellularly processed antigens that are presented by specialized proteins on the surface of the body's own cells (Guermonprez

et al. 2002). Therefore, $CD8^+$ T cells specifically recognize and kill intracellularly infected cells and eliminate pathogens that bypass antibody-mediated immunity, while $CD4^+$ T cells are known to activate other cell-types during infection (Zinkernagel and Doherty 1974a; Butz and Bevan 1998; Miller and Mitchell 1968; Heinzel et al. 1989; Bennett et al. 1998). Infections generally trigger T cell and B cell responses as their interplay is important to reach sterilizing immunity. Yet, some pathogens are more effectively eliminated by specific immune cells and intracellular infections of bacteria and viruses are particularly vulnerable to an effective $CD8^+$ T cell response. Thus, a deeper knowledge of their kinetics and effector mechanisms enables knowledge-based utilization of these cells against new and recurrent intracellular pathogens.

1.2 $CD8^+$ T cell mediated immunity

$CD8^+$ T cells are a crucial part of the adaptive immune system because they specifically recognize intracellular pathogens and can directly kill infected cells. During an immune response, a small pool of antigen specific naïve $CD8^+$ T cells undergoes massive clonal expansion to form a large amount of effector and a small population of memory $CD8^+$ T cells. Effector cells confer the immediate killing of infected cells. After resolution of the infection a high number of these cells die and memory cells persist as a reservoir for protection against reinfection (Kaech et al. 2003). The memory compartment of $CD8^+$ T cells is diverse and can be divided into functionally distinct subsets by homing markers on their surface, effector potential, recirculation routes and proliferation capacity.

Effector memory T cells (Tem) are characterized by a highly cytotoxic response to reinfection and the ability to recirculate between blood and peripheral tissues (Sallusto et al. 1999). Central memory T cells (Tcm) show a high proliferative potential and recirculate in the lymph between secondary lymphoid organs through high endothelial venules, which is mediated by CCR7 and CD62L expression (Sallusto et al. 1999). A third circulating subset, named peripheral memory T cells, surveys peripheral tissues and can enter secondary lymphoid organs by CCR7 and CD62L, but mainly uses afferent lymphatics (Gerlach et al. 2016). After the discovery of the different recirculating memory T cell subsets another subset, which resides in the tissue after infection was discovered. These tissue resident memory cells (Trm) are positioned at entry points of pathogens and are therefore a favorable local defense that can quickly resolve infection and prevent dissemination of the pathogen to other sites in the body (Mackay et al. 2012). Protection during reinfection is thought to be mediated by an interplay of all subsets and recent research has provided insights into the mechanisms of how circulating and resident memory cells cooperate to resolve infection (Ariotti et al. 2014; Beura et al. 2019). Nevertheless, key questions about the biology and recall response of Trm are to a large extent not understood. With an improved understanding of the development and behavior of these cells, they can be better induced and utilized for efficient protection.

1.2.1 Location and gene-expression define Trm

Trm are highly abundant in peripheral tissues and are thought to act as the first line of defense in barrier tissues against reinfection (Masopust and Soerens 2019). Residency was first proposed for cells that remained in the skin and root ganglia after herpes simplex virus (HSV) infection and in the small intestine after lymphocytic choriomeningitis virus (LCMV) infection (Gebhardt et al. 2009; Masopust et al. 2010). Parabiosis experiments showed a non-mixing resident memory subset between conjoined mice and microscopic analysis further substantiated the existence of Trm (Steinert et al. 2015).

To gain insight into the function of Trm and set them apart from other memory subsets a genetic core signature of Trm from lung, gut and skin was defined by microarray analysis in comparison to circulating memory cells (Mackay et al. 2013a). This reinforced the insight, that Trm do comprise a unique memory subset and are distinct from Tem, that also can recirculate through non-lymphoid tissue.

Recently, Hobit, Blimp1 and Runx3 were identified as key transcription factors that lead to Trm development (Mackay et al. 2016; Milner et al. 2017; Milner et al. 2020). On the surface Trm show a specific phenotype, that comprises markers like CD103 and or CD69 with one or both of them found on most Trm and additional organ specific markers like CD101, CD49a, PD-1 or CXCR6 (Szabo et al. 2019). During steady-state surface markers are a valuable tool to discriminate circulating from resident cells and their regulation can give insight into the differentiation and maintenance of Trm.

1.2.1.1 CD69 – a marker for activation and residency

CD69 is a dynamically expressed molecule in T cell differentiation and its role for Trm function is still under investigation. Early after $CD8^+$ T cell stimulation CD69 is upregulated and serves as an early activation marker, as CD69 protein can be detected already 2 h after activation (Simms and Ellis 1996). CD69 is a type II C lectin receptor, that was shown to be regulated by nuclear factor-κB, AP-1 and erythroblast transformation-specific related gene-1 (López-Cabrera et al. 1995). Recently CD69 was also related to tissue residency, as it can be found on many Trm in different organs (Mackay et al. 2013a).

As CD69 is an indicator for recent antigen encounter, it was thought that the maintenance of Trm could be antigen dependent. Nevertheless, in the gut the maintenance of Trm was shown to be independent of persistent antigen presentation

(Casey et al. 2012). Furthermore, “emptiness induced proliferation” of OT1 cells in lymphopenic RAG$^{-/-}$ mice resulted in similar proportions of Trm in the small intestine as after acute viral infection (Casey et al. 2012).

CD69 abundance on Trm was rather found to be linked to downregulation of tissue egress markers like S1PR1 than recent antigen encounter (Skon et al. 2013). Skon et al. showed a link of CD69 and S1PR1 expression and the transcription factor KLF2. KLF2 directly enhances expression of S1PR1 and CD62L, which promote tissue egress, but left CD69 mRNA expression levels unchanged (Bai et al. 2007). Nevertheless, overexpression of KLF2 led to a great decrease in surface expression of CD69 protein. It was concluded that KLF2 does not directly inhibit CD69 expression, but that cells with low KLF2 expression also do not express high levels of S1PR1, which engages in competitive protein-protein interactions with CD69.

Although almost all Trm express CD69 on their surface, Trm may have variant dependency on CD69 for their establishment in different organs, as knockout mice for CD69 still show homing and stable resident cells in peripheral organs (Walsh et al. 2019). Furthermore, CD69 expression was observed on CD8$^+$ T cells that were photoconverted during memory phase in the skin and left after antigen re-encounter to accumulate in draining lymph nodes (Beura et al. 2018b). Therefore, Trm may express CD69 and stably stay within tissues, nevertheless, their reaction to restimulation cannot be foreseen based solely on CD69 expression.

1.2.1.2 CD103 – a core Trm marker shaped by the tissue microenvironment

The surface molecule CD103 was defined as a key surface marker for CD8$^+$ Trm (Mackay et al. 2013b; Hardenberg et al. 2018). It binds as a dimer with integrin β7 to E-cadherin, which is expressed on epithelial cells (Hadley et al. 1997). Thereby, CD103 helps to position Trm near entry points of pathogens. The establishment of local memory depends on the recruitment of T cells into non-lymphoid tissues and their retention after the clearance of the infection. For the small intestine, T cells use α4β7 integrin and CCR9 to enter the organ. These molecules are upregulated during T cell priming in mesenteric lymph nodes and the spleen (Masopust et al. 2010). Upon arrival, T cells downregulate CCR9 and upregulate CD103, CD69 and integrin α1 (Zhang and Bevan 2013). This shift in surface molecules was attributed to a specific microenvironment including a high abundance of TGF-β, which was shown to induce CD103 expression on CD8$^+$ T cells in vitro (Kilshaw and Murant 1990), in a graft versus

host disease model and on virus activated T cells in vivo (El-Asady et al. 2005; Casey et al. 2012; Masopust et al. 2006). The influence of organ specific TGF-β signaling was emphasized by experiments showing that TGF-β receptor signaling in the spleen decreases integrin α4β7 expression in T cells and thus reduces their potential to home to the gut, whereas TGF-β receptor signaling in the gut increases tissue retention by upregulation of CD103 (Zhang and Bevan 2013). The importance of microenvironmental clues was also highlighted by transfer experiments of $CD103^+$ Trm into recipient mice, that were infected with LCMV Armstrong. The data showed that the $CD103^+$ Trm seeded into the spleen and acquired a phenotype associated with markers specific for this tissue, eventually losing the CD103 expression (Masopust et al. 2006). Yet, it exists a slight preference of homing to original tissue accompanied by seeding into various tissue locations after reinfection (Masopust et al. 2004). The flexibility of the residency phenotype was also shown in a study where CD103 expression induced by TGF-β could be overridden, by local inflammatory cytokines like IFN-β and IL-12 rendering two resident populations that express different levels of CD103 while maintaining CD69 expression (Bergsbaken et al. 2017).

The exact function of CD103 still misses the conclusive link of CD103 function beyond tissue retention. Some studies tried to target this issue by in vitro killing assays that cocultured cytotoxic $CD103^+$ $CD8^+$ T cells with target cells expressing E-cadherin (Smyth et al. 2007). In the assay antibodies that inhibited the interaction of CD103 and E-cadherin induced a reduced killing ability of $CD103^+$ $CD8^+$ T cells (Smyth et al. 2007). Another study has shown a more causal relationship of CD103 and killing as it presented that the polarization of cytotoxic granules is dependent on CD103 engagement with E-cadherin (Le Floc'h et al. 2007). In general, recent insights hint to a complex role of CD103, with an importance in Trm which goes beyond mere adhesion.

1.2.2 Trm in inflammation

To implement Trm in knowledge-based interventions to install immune protection against future infections, it is crucial to know how Trm are contributing to rechallenge and local inflammation. Recent insights characterize Trm as cells that possess the potential to rapidly react to reinfection and induce an anti-pathogenic status specific to their tissue (Ariotti et al. 2014). To achieve this, many Trm express high transcript levels of chemokines like CCL3, CCL4 and XCL1 during quiescent state and release

effector cytokines and molecules like INF-γ and GranzymeB during reinfection (McMaster et al. 2015; Schenkel et al. 2013; Mackay et al. 2016; Fernandez-Ruiz et al. 2016). Further, Trm have the ability to proliferate in situ after antigen reencounter and the local response to pathogens attracts circulating memory T cells (Beura et al. 2018a; Park et al. 2018).

Additionally, the residency status of Trm during reinfection is still under debate as certain Trm were found to stay in their organ as well as Trm characterized by CD69 expression were found in draining lymph nodes after restimulation (Beura et al. 2018b; Park et al. 2018; Behr et al. 2020). So, recent insights show that specific cells that acquired a Trm like phenotype during primary infection or during reinfection might have the ability to migrate out of the tissue.

Therefore, recent findings hint that Trm are important mediators of local immunity and may be a source for circulating memory cells. Nevertheless, further reliable evidence is needed what specific contribution to protection is uniquely based on Trm.

1.3 Aim of the study

The long-term fate of Trm and their contribution during rechallenge is currently intensively studied. Trm are largely defined by their location in tissues and retention markers on their surface. During rechallenge the clear distinction of truly resident cells and cells that immigrate into the tissue becomes increasingly difficult.

The aim of this study is to establish highly specific models and methods that clearly mark Trm and enable fate-mapping of Trm, establish a quantitative imaging approach to observe immune cells in situ and investigate the specific contribution of Trm during reinfection.

The first objective is to confirm the specificity of two fate-mapping models for Trm based on common Trm markers. The model is based on the inducible ER^{T2}-Cre, which is either controlled by CD69 or CD103 expression and excises a floxed STOP codon in front of different fluorescent reporter genes. This enables fate-mapping of Trm. Figure 1 shows an example for the fate-mapping system based on CD103 expression.

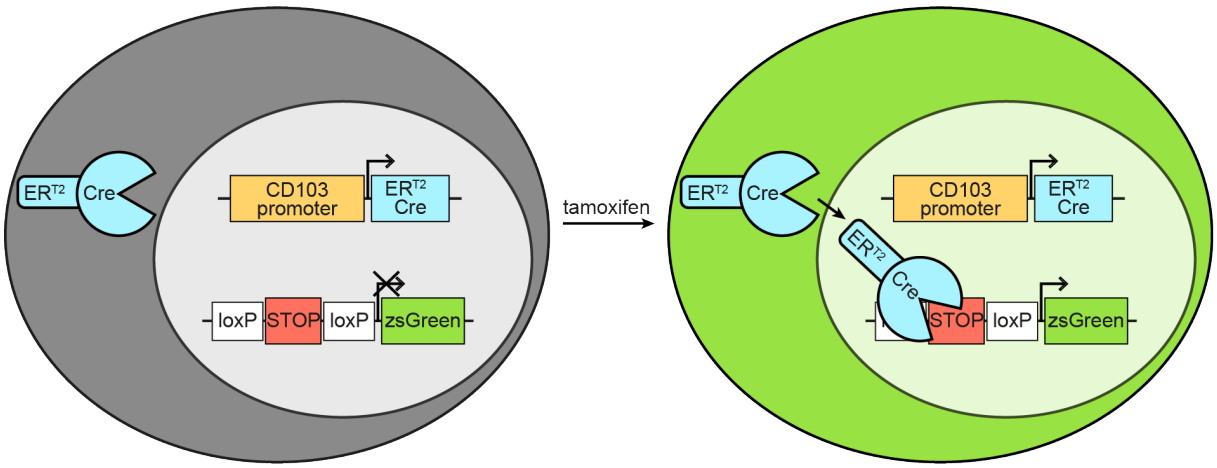

Figure 1: **Illustration of reporter system for the example of CD103 driven expression of zsGreen.** CD103 expression drives ER^{T2}-Cre expression. After tamoxifen administration, ER^{T2}-Cre can translocate to the nucleus and excise the STOP codon in front of zsGreen. This leads to a permanent, temporally controlled labelling of the cell.

The second objective is to establish a Trm specific rescue system, that eliminates the circulating memory compartment and leaves the $CD103^{+}$ Trm population intact. The system is based on the insertion of a floxed diphtheria toxin receptor (DTR) into the genome of mice, which can be excised by CD103 driven ER^{T2}-Cre. This enables

the specific rescue of CD103⁺ Trm after tamoxifen application, as the floxed DTR is excised and the cells do not die after DTX exposure, as seen in figure 2

.

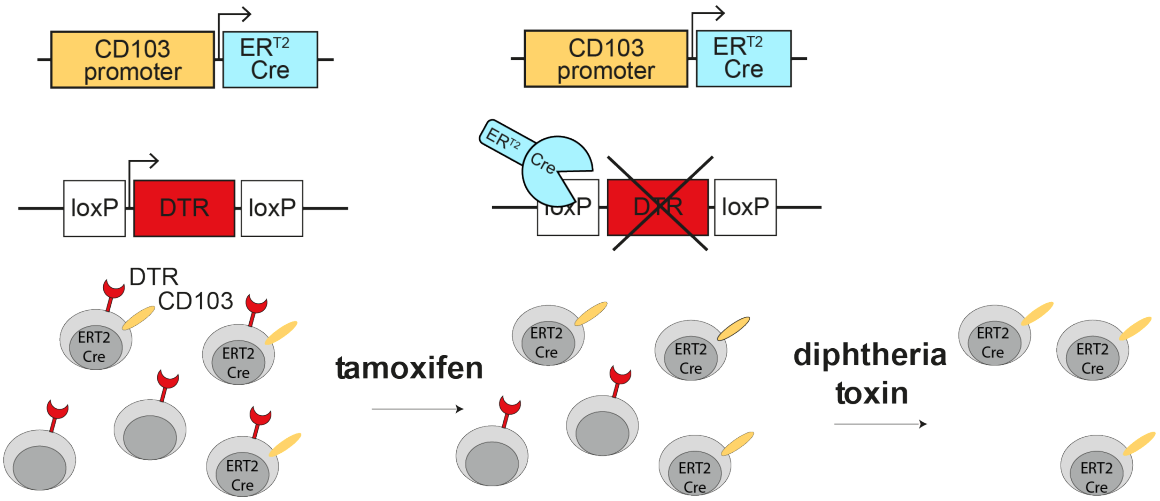

Figure 2: **Rescue system for Trm.** CD103⁺ Trm are rescued from DTX induced cell death by excision of the floxed DTR by a CD103 driven ER^{T2}-Cre.

The third objective is the setup of a quantitative imaging method, that enables the visualization of cells in tissues and an unbiased assessment of their interaction and location.

The last objective is to delineate the behavior of Trm during rechallenge. Therefore, Trm are phenotypically, numerically, and genetically analyzed.

In conclusion, this work aims to characterize the behavior of Trm in steady state and during reinfection with a temporally tightly controlled and cell subset specific fate-mapping system. Further, it presents a valuable rescue model for Trm and an unbiased imaging approach, which can be used to delineate specific functional contributions of Trm during rechallenge.

Chapter 2

Methods

2.1 Mice

2.1.1 Host mice

To study T cell function in vivo C57BL/6 mice (Bl6 mice) obtained from Charles River were generally used as hosts for transfer experiments. Vβ5 TCRβ only transgenic mice obtained by P. Fink were used if a risk of rejection of the transferred cells due to e.g. reporter expression was expected (Dillon et al. 1994).

2.1.2 Transgene models to study cell function

Biotechnological methods enable the engineering of TCR specificity, cell type specific and temporally controlled activation of reporter genes or rescue of certain cell types. This allows fate-mapping of cell subsets and attribution of specific functions to single cell subsets. The basis of gene specific and temporal control are modified enzymes like ER^{T2}-Cre which can be combined with TCR transgenes, reporter genes or rescue systems.

2.1.2.1 TCR engineered mice and reporter mice

TCR transgenic mice are a useful tool to study T cell responses in vivo, as they allow easy tracing of antigen specific cells. OT-1 TCR transgenic mice recognizing the peptide Ova257-264 from OVA were obtained from Jackson Laboratory (Bar Harbor, Maine, USA) (Hogquist et al. 1994). P14 TCR transgenic mice recognizing the peptide gp33-41 of LCMV were provided by A. Oxenius (ETHZ, Switzerland) (Pircher et al. 1990). Reporter mice Ai6(RCL-ZsGreen), R26-stop-EYFP, Ai14 (RCL-dtomato) and $Nur77^{GFP}$ were also obtained from Jackson Laboratory.

2.1.2.2 ER^{T2}-Cre based fate-mapping and rescue mice

The mouse strains CD103-ER^{T2}-Cre and CD69-ER^{T2}-Cre were generated by usage of a BAC containing the entire coding sequence for Cre and ERT2, including a linker and a final SV40 poly(A) sequence downstream of a CD103-5´-UTR or CD69-5´-UTR, respectively. Pronuclear injection was performed by the Institut Clinique de la Souris and the Mouse Clinical Institute (MCI) (Alsace, France).

Cre recombinase is a 38 kDa protein from bacteriophage P1, that can mediate excision, inversion and translocation of DNA, depending on the orientation of loxP sequences on the DNA strand (Sauer and Henderson 1988). The sequence of Cre was modified to enhance expression efficiency by codon optimization and reducing CpG content (Shimshek et al. 2002). In settings where tight temporal control over DNA excision events is necessary, ER^{T2}, a triple mutated estrogen receptor, is fused to Cre (Feil et al. 2009). Thereby, without binding of synthetic estrogen receptor ligand 4-hydroxytamoxifen (OHT) to ER^{T2}, Cre cannot translocate to the nucleus. When OHT is applied the fusion protein can enter the nucleus and Cre can mediate the excision. In vivo mice are treated with tamoxifen and liver enzymes convert it into the active metabolite OHT (Whitfield et al. 2015).

For the mouse strain DTR-loxp a BAC containing the floxed human Diphtheria toxin receptor with a SV40 poly(A) sequence under the control of a Rosa promoter was generated and pronuclear injection was performed in the Karolinska Institutet Mouse Models (Karolinska Center for Transgene Technologies Comparative Medicine, Karolinska Institutet Stockholm, Sweden).

Diphtheria toxin (DTX) is produced by *Corynebacterium diphtheriae.* It is composed of DTX-A and DTX-B, with DTX-B mediating internalization into cells by receptor mediated endocytosis (Tsuneoka et al. 1993; Draper and Simon 1980). The acidic conditions in the late endosome lead to the entry of DTX-A into the cytosol, where it inhibits protein synthesis by inactivating elongation factor 2 (Sandvig and Olsnes 1980; Saito et al. 2001). The diphtheria toxin receptor (DTR) is the membrane bound form of the heparin-binding EGF-like growth factor (Schneider and Wolf 2009; Naglich et al. 1992). In rats and mice the receptor comprises amino-acid changes, that renders their cells 10^5 times less susceptible to DTX than human cells (Mitamura et al. 1995; Pappenheimer et al. 1982). Therefore, inserting the simian DTR in mouse cells restores their sensitivity to DTX and creates a tool for ablating specific cell types.

There are two ways to use the DTR-DTX system to ablate cells. Either a specific cell type is targeted by DTX, which has been done for example for regulatory T cells (Tregs) (Kim et al. 2007). The DTR was inserted into the 3' untranslated region of Foxp3, a vital factor for Tregs. After DTX application Tregs were depleted, and mice developed autoimmune disease. Therefore, the model helped to gain insight in immune regulation by Tregs. The other approach is to use a floxed DTR, that is expressed in all cell types, but not in Cre expressing cells. This was first done by gene targeting of embryonic stem cells in Terminator mice, which have the floxed DTR knocked into the Rosa26 locus (Guo et al. 2013). This approach helped to obtain pure primary culture cell subsets from various organs, because cells of interest expressed Cre and thus protected desired cells from ablation by DTX. Here only the variant with the floxed simian Diphtheria toxin receptor was used.

All BACs were generated by Gene Bridges (Heidelberg, Germany). Mice were bred, maintained, and infected in specific pathogen-free facilities of the Technical University of Munich.

Experiments were performed in male or female mice that were at least six weeks old in compliance with the institutional and governmental regulations in Germany and were approved by the responsible veterinarian authorities of the Regierung von Oberbayern in Germany.

2.2 Tamoxifen preparation and administration

Tamoxifen was dissolved in corn oil at a concentration of 20 mg/ml by shaking the solution for 1 h in the dark at 37 °C. Mice received 100 mg/kg tamoxifen by intraperitoneal injection (i.p.). For in vitro applications, the active component of tamoxifen OHT was used at a concentration of 500 ng/ml.

2.3 Diphtheria toxin preparation and administration

Diphtheria toxin was solved in PBS at a concentration of 2mg/ml. The mice were given 50 µg/kg by i.p. injection.

2.4 Infections

2.4.1 Listeria monocytogenes

Listeria monocytogenes (Lm) is a gram-positive bacterium, that can infect phagocytic and non-phagocytic cells intercellularly. Thereby, proteins from the bacteria end up on MHC class I complexes and elicit $CD8^+$ T cell immune responses. Lm enters cells inside a vacuole, which it escapes with the help of Listeriolysin O (Bielecki et al. 1990). To infect other cells intercellularly it polymerizes actin by applying actin assembly-inducing protein (ActA) (Kocks et al. 1992). These proteins have been genetically removed to modify the motility of certain Lm strains (Chakraborty et al. 1995; Cossart et al. 1989). Further genetic manipulations resulted in Lm strains that express various antigens, like the chicken egg protein ovalbumin (OVA) or parts of the LCMV (Zehn et al. 2009; Oberle et al. 2016).

Lm is a food borne pathogen in humans. Yet, mice differ in the sequence for E-cadherin on intestinal cells, which impairs the binding of the virulence factor internalinA, which is crucial for entry into the host. This renders mice less susceptible for oral Lm infection (Bergmann et al. 2013). Lm is thus widely administered to mice by intravenous injection, which creates a model system to study pathogen clearing by innate and adaptive immune mechanisms (Lewis et al. 2019). Early during infection innate immune cells like neutrophils, monocyte derived TIP-DCs and macrophage populations control Lm growth in marginal zones (MZ) of the spleen (Serbina et al. 2012; Witter et al. 2016; Waite et al. 2011). $CD8a^+$ DCs are subsequently crucial to initiate a $CD8^+$ T cell response, while also contributing to Lm propagation in the white pulp (WP) (Edelson et al. 2011). It was shown, that $CD169^+$ macrophages trans-infect $CD8a^+$ DCs in the MZ and thereby promote Lm shuttling to the white pulp (Perez et al. 2017). $CD8^+$ T cells are required for sterilizing immunity against Lm, as SCID-mice, which lack lymphocyte immunity, develop a chronic Lm infection (Bhardwaj et al. 1998).

The growing knowledge about Lm biology further encourages the use of this model pathogen to address questions like vaccine design and therapy approaches for inflammatory diseases (Pamer 2004).

Here recombinant Lm strains stably expressing OVA or the peptide gp33-41 of LCMV were used (Zehn et al. 2009; Oberle et al. 2016). To infect mice orally with Lm-OVA, a murinised InternalinA (Lm-OVA-Ina_mut) variant was generated. Therefore,

E.coli carrying the plasmid pPL2 containing the murinised InternalinA were conjugated with Lm-OVA (Wollert et al. 2007).

Frozen stocks of Lm strains were thawed and grown at 37 °C in BHI-medium to log phase. Bacterial numbers were determined by measuring the OD at 600 nm. Naïve mice received 1000-2000 colony forming units (cfu) intravenously (i.v.) and previously infected mice received $5x10^6$ cfu of Lm-OVA or Lm-gp33. For rechallenge with Lm-OVA-Ina_mut 10^9 cfu were orally gavaged.

2.4.2 VSV

VSV belongs to the Rhabdoviridae and is an RNA virus, which primarily infects rodents, cattle, swine and horses (Lichty et al. 2004). It acts highly cytopathic, which favors antigen uptake by antigen presenting cells (APC) from cell debris and thereby cross-presentation to $CD8^+$ T cells (Cobleigh et al. 2012). The most important serotypes are New Jersey and Indiana, which are differentiated by distinct neutralizing antibodies against their surface glycoprotein and vary in their pathogenesis, with New Jersey strains leading to more severe outbreaks (Martinez and Wertz 2005). The surface glycoprotein binds to phosphatidylserine, which is expressed on almost all animal cells. It fuses the viral and host cell membranes, enabling infection of a broad range of cells (Lichty et al. 2004). The virus was genetically modified to carry various antigens from pathogens like influenza or HIV or model antigens like OVA (Lichty et al. 2004). The VSV-OVA model showed that antigen after VSV infection is presented for a longer period than expected from a classical acute virus strain, leading to activation of antigen specific cells weeks after primary infection (Turner et al. 2007). Together, VSV can be used to study $CD8^+$ T cell responses to a broad variety of antigens.

Here VSV-gp33, which was previously generated in the lab and VSV-OVA were used. They were grown and titrated on BHK-21 cells (Kim et al. 1998). Mice were infected i.v. with $4x10^6$ pfu and $2x10^6$ pfu, respectively.

2.4.3 LCMV

LCMV is a member of the Arenaviridae and has two negative-sense single-stranded RNA segments (Lee et al. 2000). It naturally infects rodents, but can also infect humans (Zhou et al. 2012). The virus comprises variants that differ in their course

of disease (Ahmed and Oldstone 1988; Bergthaler et al. 2010). LCMV-Armstong (LCMV-Arm) elicits a strong immune response and is cleared within two weeks. LCMV-clone13 (LCMV-c13) shows persistence, although only three amino acids are changed (Beura et al. 2015; Salvato et al. 1988; Matloubian et al. 1993). Several peptides from LCMV are immunodominant with gp33 being presented in the H-2Db context to $CD8^+$ T cells (Siddiqui and Basta 2011; Puglielli et al. 2001). The virus is non-cytopathic, which means that the cytolytic activity during immune response is due to the host immune system. LCMV was used in studies that discovered MHC restriction of T cells and as a model antigen to study PD-1 blockade (Blattman et al. 2009; Zinkernagel and Doherty 1974b). Therefore, the virus is a valuable tool to study acute and chronic $CD8^+$ T cell responses.

Here 2×10^5 plaque forming units (pfu) LCMV Armstrong (generated from infected Vero cells provided by M. J. Bevan) were injected i.p. into the mice.

2.5 Purification of T cells for adoptive transfer

Spleens were mashed through a 100 µm cell strainer. After centrifugation at 400 x g for 4 minutes (min) the supernatant was discarded and the pellet resuspended in 1 ml ACK-buffer, to eliminate red blood cells. $CD8^+$ T cells were collected with the CD8a+ T Cell Isolation Kit according to manufacturer's instructions. The $CD8^+$ T cells were then injected in mice or used for cell culture.

2.6 Preparation of single cell suspensions from spleen and thymus

Single cell suspensions were obtained as described above for adoptive transfer. After the ACK lysis the cells were plated in a round bottom 96 well plate for flow cytometric staining.

2.7 Preparation of single cell suspensions from liver

When the liver was harvested, mice were perfused with 5-10 ml PBS. Organs were mashed through a 100 µm cell strainer. After centrifugation for 10 min at 500 g the pellet was resuspended in 35 % percoll. By centrifugation for 20 min at 500 g at room temperature (RT) and no brake, density gradient centrifugation separates epithelial

and dead cells on top of the percoll and erythrocytes and lymphocytes on the bottom. After ACK lysis of erythrocytes (1 ml, 2 min) the suspension was centrifuged again for 5 min at 500 g. After decanting the supernatant, cells were plated in a round bottom 96 well plate.

2.8 Preparation of single cell suspensions from small intestine

11 cm of the small intestine lamina propria (SI-LP) were harvested beginning from the stomach. Then all Peyer's patches were removed, and the organ cut open and washed in PBS. Afterwards, it was transferred to a 50 ml falcon containing cleaning buffer for the small intestine. Next, the tube was shaken vigorously for 20 s and the tissue was washed again with PBS. Digestion solution for each small intestine was put into 50 ml tubes and the organ was further cut into small pieces. After 15 min of incubation at 37 °C at 290 rpm the suspension was pipetted up and down with a 10 ml pipette. This was done 2 more times with an incubation period of 20-30 min, depending on the digestion result. Consequently, the whole digestion volume was filtered into 50 ml tubes and centrifuged at 550 g for 7 min. The pellet was resuspended in 5 ml 44 % percoll and underlaid with 67 % percoll and centrifuged for 15 min at 1600 g at RT without brakes. The gradient separates the epithelial and dead cells on top, the lymphocytes in the interphase of the percoll layers and the erythrocytes at the bottom. After collecting the interphase, the suspension was centrifuged at 500 g for 5 min at RT. Following decanting the supernatant, cells were plated in a round bottom 96 well plate.

2.9 Preparation of blood for flow cytometric staining

50 µl blood was mixed with 20 µl heparin (5000 U/ml) in a 96 well plate or for infected mice in 1.5 ml eppendorf tubes to prevent clotting. Then red blood cells were lysed using 200 µl or 1 ml ACK-buffer, respectively. After incubation of 5 min at RT, the plate or tubes were centrifuged at 400 g for 1 min or 500 g for 5 min. The supernatant was decanted, and the pellet resuspended in ACK-buffer and spun down, as above. The cells in the tubes were then transferred into a round bottom 96 well plate. Then, all cells were washed with 100 µl FACS-buffer and centrifuged as above. Then the cells were stained for flow cytometric analyses, described below.

2.10 In vitro culture

For cultivation of the $CD8^+$ T cells, they were seeded in RPMI-medium containing 10 % FCS and medium supplement. 50 U/mL IL-2 and 30 µL pre-washed CD3/CD28 Dynabeads were added. The cells were incubated at 37 °C and 7 % CO_2. Culture volumes were increased as needed. 50 U/mL IL-2 was added on every other day.

2.11 Antibody staining for flow cytometric analysis

Single cell suspensions were plated in a round bottom plate, like described above. Then the cells were centrifuged at 500 g for 1 min at RT and the supernatant decanted. Subsequently, to avoid unspecific antibody binding anti CD16/CD32 antibody (clone 2.4G2) was applied in 50 µl FACS-buffer. After incubation of 10 min at 4 °C, antibodies were applied in appropriate concentrations in 50 µl FACS-buffer for 20-30 min at 4 °C. Then, the cells were washed with 100 µl FACS-buffer and centrifuged as above and the supernatant decanted. To fix the cells, fixation-buffer was applied for 30 min at 4 °C. After washing and centrifuging the cells again, they were either resuspended in 100 µl FACS-buffer for flow cytometric analysis or washed again and resuspended in 100 µl permeabilization-buffer and spun down for intracellular staining. Then, the cells were resuspended in 200 µl permeabilization-buffer and incubated for 10 min at RT. After centrifuging, the pellet was resuspended in 100 µl permeabilization-buffer containing the appropriate antibodies and incubated for 40 min at 4 °C. Then the cells were washed twice in permeabilization-buffer and finally taken up in 100 µl FACS-buffer for flow cytometric analysis.

2.12 Next-generation sequencing

2.12.1 Sample processing

Next-generation sequencing was performed as described in Alfei et al. (Alfei et al. 2019). At day 2 after reinfection or during memory phase, SI-LP cells were enriched for $CD45.1^+$ OT1 using biotin-labelled anti-CD45.1 antibodies and anti-biotin-conjugated microbeads in combination with magnetic MACS cell separation. $CD103^+zsGreen^+$, $CD103^+zsGreen^-$ and $CD103^-zsGreen^-$ cells were then obtained by flow cytometry-based sorting of $CD45.1^+$ OT1. The cells were lysed and RNA was extracted using the Agencourt RNAdvance Cell v.2 kit. cDNA synthesis and PCR

amplification using 9,5 µl of each RNA sample was performed using SMART-Seq v.4 Ultra Low Input RNA Kit for Sequencing. After cDNA synthesis, each sample was subjected to 14 cycles of PCR amplification. Then, 5 µl of the resulting amplified cDNA was used for library preparation with the Illumina Nextera XT DNA Library reagents. After PCR amplification of the fragmented libraries, the samples were purified with (0.6x) Agencourt AMPure XP beads and eluted in 10 µl of molecular-grade water. The quality of the resulting library was assessed with the use of Agilent High Sensitivity DNA Kit. The library quantification was performed based on the Illumina recommendations (SY-930-1010, Illumina) with the use of KAPA SYBR FAST qPCR Master Mix. The samples were sequenced on Illumina HiSeq 2500 system with the following conditions: rapid run, 100-bp single-end reads, dual-indexed sequencing, resulting in 20 million reads per sample.

2.12.2 Data processing

Reads were processed using snakemake pipeline41 v.0.1 as indicated at https://gitlab.lrz.de/ImmunoPhysio/bulkSeqPipe. Sequencing quality was assessed with fastqc42, filtering was performed by trimmomatic v.0.3643, mapping by STAR v.2.5.3a44 with genome Mus_musculus.GRCm38, counting by htseq v.0.9.145 with annotation Mus_musculus.GRCm38.91. To supervise STAR and fastqc results, multiqc v.1.246 was used.

Differential expression analysis was performed with methods based on the negative binomial distribution in DESeq2 (v.1.18.1)47, using default parameters. Read counts were modelled as a negative binomial distributions with estimated mean values and gene-specific dispersion parameters; each gene was fitted as a generalized linear model. Wald statistics and the Benjamini and Hochberg correction were used for significance tests and multiple comparisons.

2.13 Cryosectioning and immunofluorescence staining

For cell detection in situ, organs were harvested in a 4 % formaldehyde solution and incubated for 4 h at 4 °C. Then, they were put into a 30 % sucrose solution over night at 4 °C. The organs were frozen over liquid nitrogen, embedded in OCT-medium and stored at -80 °C. Then, they were cut into 5 µm thin slices with a cryotome and mounted on superfrost slides. After dehydrating for 3 min in cold acetone, the organ

slices were then either frozen at -20 °C or immediately used for staining. Therefore, the slices were rehydrated with PBS in a humid chamber to avoid that the slides run dry. Then, the slices were circled with a PAP pen to minimize the staining volume. After washing with PBS, Avidin/Biotin solution was added according to manufacturer's protocol. After washing, 50 µl PBS containing the appropriate antibodies was added and the slices were incubated over night at 4 °C. Then the slides were washed for 5 min in PBS and, if a secondary antibody was used, incubated in 50 µl PBS containing the appropriate antibody. To stain for DAPI, subsequently 1 µg/ml DAPI solution was added, incubated for 5 min and then the slices were washed again. Then, excess of liquid was removed, and one drop of Prolong Gold mounting buffer was applied on each slice. Further the slide was topped by a cover glass and stored in the dark until analysis under the Leica DMi8 fluorescent microscope.

Chapter 3

Results

3.1 Development of methods to assess local immune responses

Immune cells reside and function largely in lymphoid and non-lymphoid tissues. An improved understanding of the mechanisms that govern local immune responses is therefore crucial for understanding specific roles of resident versus non-resident cells.

As tissues are in constant interchange with circulating cells it is hard to determine a true residency status of a cell only by its location. Therefore, resident specific gene expression allowed to find markers that only Trm share during steady state. Nevertheless, tracing of Trm during and after reinfection traditionally poses a challenge, as surface markers that define Trm overlap with transiently expressed activation markers and tissue retention molecules. Therefore, two reporter systems based on widely accepted Trm specific surface markers were developed to fate-map Trm. In the following the specificity of the fate-mapping models is validated. The CD103 based model allowed faithful Trm labelling and is therefore a useful tool to study Trm behavior during reinfection.

In addition, a complementary rescue model was implemented that specifically installs $CD103^+$ Trm before reinfection to distinguish their functional contribution to protection. This model was tested on $CD103^+$ Trm specificity and proved to be a tool with great potential to describe Trm function.

To further allow a detailed analysis of cells in tissues, a quantitative imaging system was additionally developed, that allows an unbiased cell identification in the tissue and the analysis of cell-cell interaction. This system was validated in different infections and several organs to prove its functionality.

3.1.1 Development of fate-mapping mouse models for Trm

To assess the function of Trm and molecular mechanisms that govern Trm behavior, transgenic lineage tracing mouse models were developed. CD69 and CD103, two Trm surface markers, were chosen to trace Trm during steady state and after reinfection. The fate-mapping approaches are based on a BAC-construct containing the CD69 or CD103 promoter before the Cre recombinase. To be able to confine Cre activity to a certain time window, ER^{T2}-Cre was chosen, which can be activated by tamoxifen treatment.

The CD103 based fate-mapping model proved to be highly specific and faithful for Trm tracing, while the CD69 model was not reporting Trm. In the following, the validation of both constructs is described.

CD103 and CD69 are classical Trm surface markers that discriminate Trm from circulating cells during steady state. During reinfection though, CD103 is upregulated by newly tissue infiltrating cells and CD69 is acquired by recently activated circulating cells. To meet the challenge to discriminate Trm from recently activated or tissue infiltrating cells CD103 and CD69 fate-mapping mouse models were generated. The models are based on transgenic mice that were generated by pronuclear injection of two BACs, which contain either a CD103 or a CD69 promoter driven ER^{T2}-Cre (CD103-ER^{T2}-Cre or CD69-ER^{T2}-Cre mice). Both models were validated for specificity to report Trm.

To allow reporter expression, CD103-ER^{T2}-Cre mice were crossed to loxp-STOP-loxp-zsGreen mice (CD103-zsGreen-reporter mice). Further they were crossed to obtain the T cell receptor specific for the H-2Db restricted peptide gp33-41 of LCMV or the H-2Kb restricted ovalbumin peptide residues 257-264 (CD103-zsGreen-reporter-P14 mice and CD103-zsGreen-reporter-OT1 mice), as shown in figure 3A.

CD69-ER^{T2}-Cre mice were crossed to either loxp-STOP-loxp-YFP or loxp-STOP-loxp-dTomato mice to find optimal recombination conditions for fluorescent reporter expression (hereafter, CD69-YFP-reporter mice, or CD69-dTomato-reporter mice). Additionally, these mice were crossed to obtain the T cell receptor specific for the H-2Db restricted peptide gp33-41 of LCMV (CD69-YFP-reporter-P14 mice or CD69-dTomato-reporter-P14 mice). An illustration of the CD69 fate-mapping mouse can be seen in figure 3B.

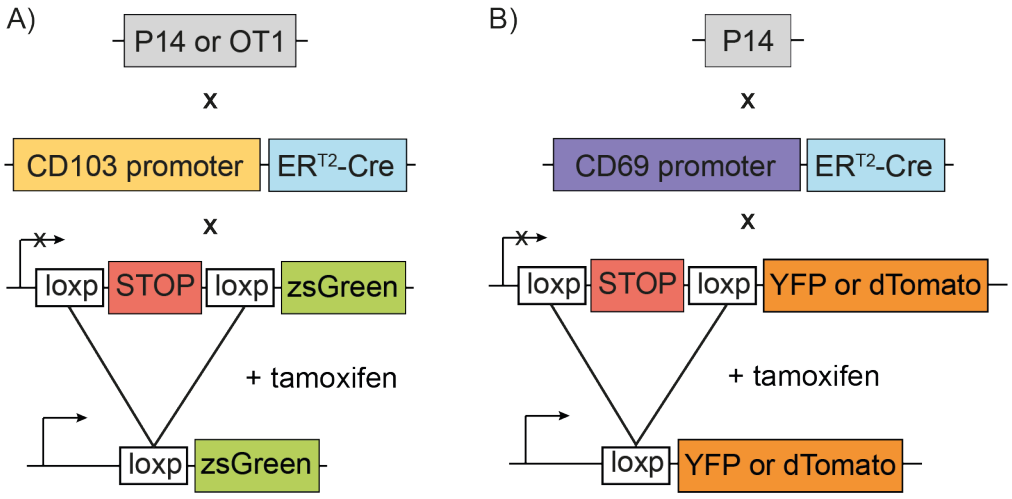

Figure 3: **Graphical illustration of the Fate-mapping systems.** P14 or OT1 mice were crossed to A) CD103-reporter mice or B) CD69 reporter mice, which carry a A) CD103 or B) CD69 promotor driven ER^{T2}-Cre. Further, the mice carry a floxed STOP-codon in front of a fluorescent reporter gene (A: zsGreen, B: YFP or dTomato). Tamoxifen leads to translocation of ER^{T2}-Cre to the nucleus, where it excises a STOP-codon, allowing fluorescent reporter transcription.

The microinjection of BAC DNA resulted in 6 different founder mice for the CD103 construct, which differed in their efficiency of the excision of the STOP codon in front of the reporter zsGreen and therefore the expression of the reporter (data not shown). For the CD69 construct the microinjection of BAC DNA yielded only one founder.

3.1.1.1 Validation of CD103 fate-mapping model

First, the CD103 fate-mapping model was tested for its ability to report CD103 surface protein. CD8$^+$ T cells naturally express CD103 in the thymus, SI and in naïve mice also in the spleen. Therefore, to test the ability of the CD103 fate-mapping model to display CD103 expression, transgenic CD103-zsGreen-reporter mice received tamoxifen twice and organs were harvested 2 days later (Figure 4).

In tissues, where cells are known to express high levels of CD103, like thymus and SI, they expressed the reporter and the expression correlated well with CD103 protein on the surface. Reporter positive cells could also be found in spleen and blood. In spleen reporter expression resembled low CD103 expression, while in the blood CD103 was already downregulated. The good correlation between CD103 protein levels and reporter expression led to the conclusion, that in the CD103-zsGreen-reporter mice CD103 expressing cells can be faithfully labeled.

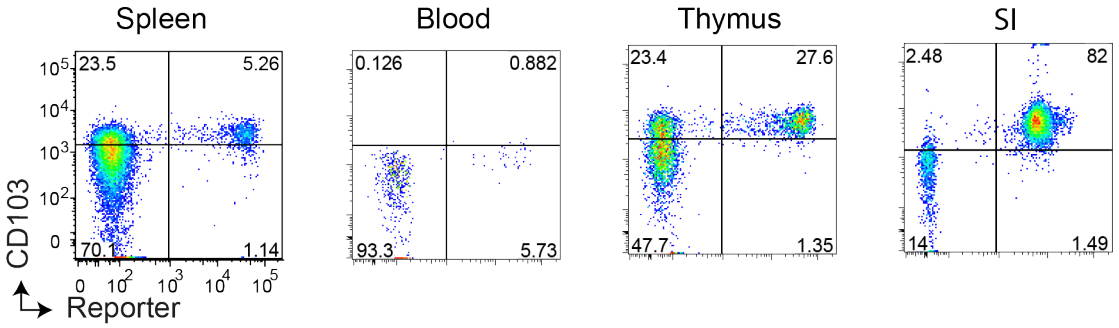

Figure 4: **Reporter expression reflects CD103 expression in various tissues**. CD103-zsGreen-reporter mice received 100mg/kg tamoxifen on d0 and d1. On d4 they were sacrificed, and the organs harvested. Shown are representative flow cytometry plots showing reporter zsGreen and CD103 expression.

The aim for the generated reporter mouse is to trace Trm. Therefore, the next step was to verify the reporter expression in a setup containing memory cells. Hence, $CD8^+$ T cells from a CD103-zsGreen-reporter-P14 or CD103-zsGreen-reporter-OT1 mouse were transferred into Bl6 mice. Mice were infected with different pathogens, that were either genetically modified to carry the antigen OVA or gp33 or are naturally expressing the antigen. Tamoxifen was administered during memory phase. In figure 5 memory CD103-zsGreen-reporter cells are shown from different infections in the SI-LP, as Trm are known to express CD103 at this location. While an infection with OVA containing antigen resulted in a more robust Trm population in the SI compared to Lm-gp33 and VSV-gp33, the percentages for double positive cells for reporter and CD103 expression are similar. Trm generated by LCMV-Arm are the exception, which yielded a strong Trm population with an about two times higher reporter positive cell frequency.

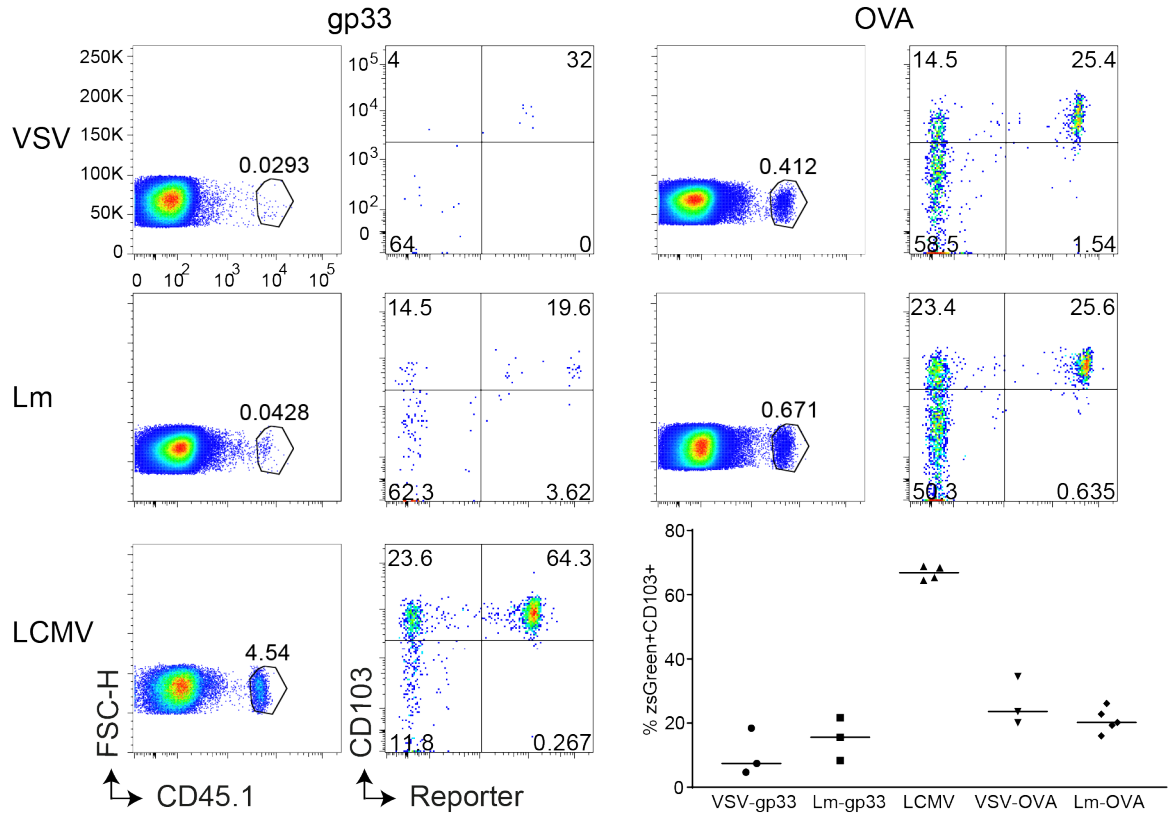

Figure 5: **Reporter construct specifically labels CD103⁺ cells during memory phase in the SI**. 5000 P14 or OT1 CD103-zsGreen-reporter cells were transferred into Bl6 mice. The mice were infected with either VSV-gp33 ($4x10^6$ pfu), VSV-OVA ($2x10^6$ pfu), Lm-gp33 (1000 cfu), Lm-OVA (1000 cfu) or LCMV-Arm ($2x10^5$ pfu). Between d26 and d37 100mg/kg tamoxifen was administered twice to the mice. The CD103-zsGreen-reporter population was assessed in the SI between 3 and 20 days after tamoxifen treatment. P14 and OT1 populations determined by CD45.1 expression are shown. Further, CD103 and reporter expression are shown in representative flow cytometry plots. Percentages of zsGreen⁺ CD103⁺ cells of transferred cells are shown.

The reporter correlated strongly with CD103 expression and was mainly found in tissues with Trm occurrence like the SI-LP, lung and skin (Figure 5, data not shown). Also, the spleen was analyzed for the occurrence of reporter positive cells (Figure 6).

Only for VSV-OVA a small population of reporter positive cells could be detected in the spleen, while in other infections virtually no reporter expression could be observed.

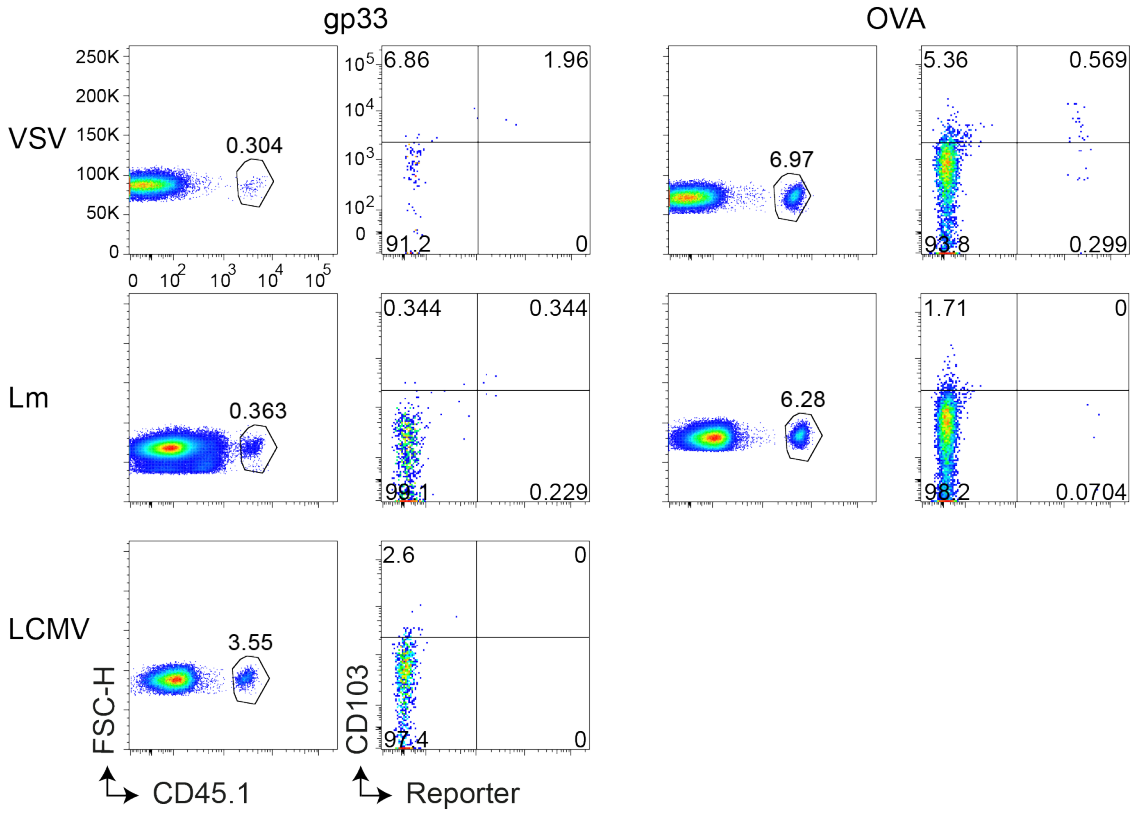

Figure 6: **Reporter construct shows practically no unspecific labelling in spleen.** 5000 P14 or OT1 CD103-zsGreen-reporter cells were transferred into Bl6 mice. The mice were infected with either VSV-gp33 ($4x10^6$ pfu), VSV-OVA ($2x10^6$ pfu), Lm-gp33 (1000 cfu), Lm-OVA (1000 cfu) or LCMV-Arm ($2x10^5$ pfu). Between d26 and d37 100mg/kg tamoxifen was administered twice to the mice. The CD103-zsGreen-reporter population was assessed in the spleen between 3 and 20 days after tamoxifen treatment. P14 and OT1 populations determined by CD45.1 expression are shown. Further, CD103 and reporter expression is shown in representative flow cytometry plots.

To further verify that the $CD103^+zsGreen^+$ CD103-zsGreen-reporter cells have a Trm phenotype in the SI-LP, the cells were analyzed for common markers to differentiate memory cell populations like CD69, CX3CR1 and CD62L (Figure 7).

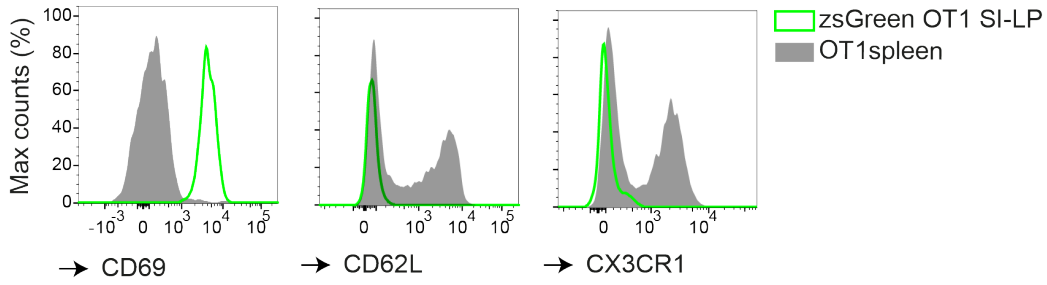

Figure 7: **Reporter⁺ cells show a Trm phenotype.** 5000 CD103-zsGreen-reporter-OT1 cells were transferred into Bl6 mice on d-1. The mice were infected on d0 with 1000 cfu Lm-OVA. On d24 and d25 100mg/kg tamoxifen was administered. The transgene memory population was assessed on d41. Representative histograms for the expression of CD69, CD62L and CX3CR1 for CD103⁺zsGreen⁺ CD103-zsGreen-reporter-OT1 cells from SI-LP and CD103⁻ zsGreen⁻ CD103-zsGreen-reporter-OT1 cells from the spleen are shown.

CD103-zsGreen-reporter-OT1 cells that expressed CD103 and zsGreen showed a high expression of the Trm marker CD69 and low expression for the Tcm marker CD62L and Tem marker CX3CR1 (Figure 7).

To conclude, the reporter construct reports highly specifically Trm in peripheral organs and shows limited leakiness in organs without CD103 expression.

3.1.1.2 Validation of CD69 fate-mapping model

CD69 is a marker that is found on Trm and upon stimulation naïve CD8⁺ T cells upregulate CD69 on their surface. To determine if reporter expression correlates with CD69 protein levels in a time efficient way, reporter expression was assessed on day 7 after activation, as all naïve cells should upregulate CD69 after activation and therefore be reporter⁺. So, Bl6 host mice received CD8⁺ T cells from CD69-YFP-reporter P14 mice or CD69-dTomato-reporter P14 mice and were infected with LCMV-Arm. Tamoxifen was administered before and early during infection. In figure 8 the expression of the reporter proteins and CD69 expression for the two different donor strains (YFP or dTomato) are shown on day 7.

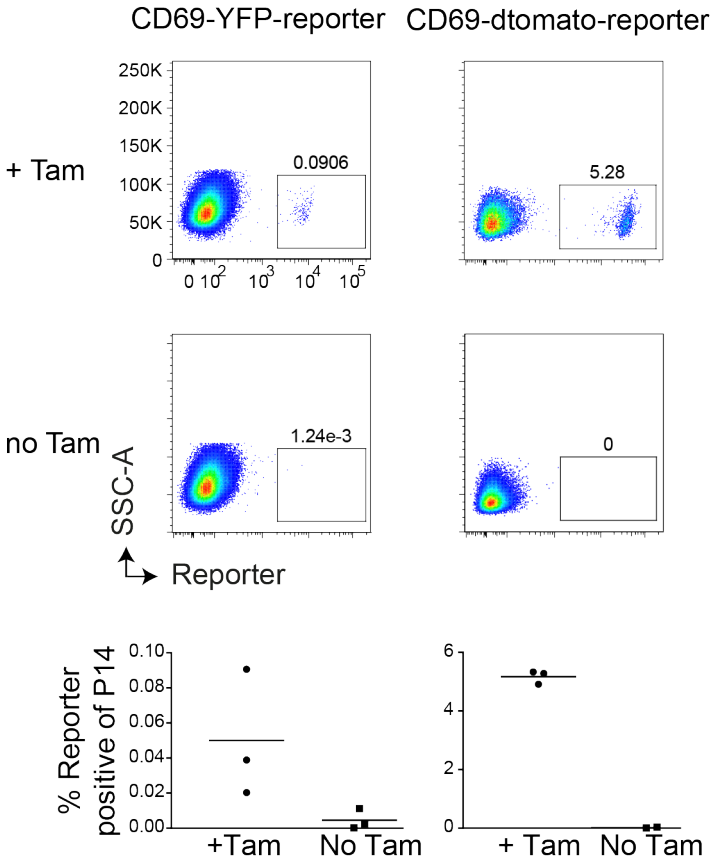

Figure 8: **CD69 dependent reporter expression can be observed in vivo.** Bl6 mice received either CD69-YFP-reporter or CD69-dTomato-reporter CD45.1^{+} P14 cells before i.p. infection with 2x10^{5} pfu LCMV-Arm. Mice received 100 mg/kg tamoxifen for 3 days from d-1 to d1. Shown are representative plots for reporter expression and percentages of reporter positive cells of splenocytes on d7 after infection.

CD69-dTomato-reporter P14 had a 10-fold higher frequency of reporter positive cells compared to CD69-YFP-reporter donors. Nevertheless, the expression of about 5 % of all dTomato-reporter donor cells was still much lower than expected, as CD69 is universally expressed on activated cells. Due to the 10-fold higher frequency of reporter positive CD69-dTomato-reporter donors, these mice were chosen for further experiments.

To better compare the correlation of CD69 and the reporter protein expression and to define the system during memory stage of an infection, the time of analysis was chosen 28 days after infection. To avoid rejection of the donor cells Vb5 mice were chosen as hosts. Mice received 10000 CD69-dTomato-reporter P14 cells and were infected with LCMV-Arm.

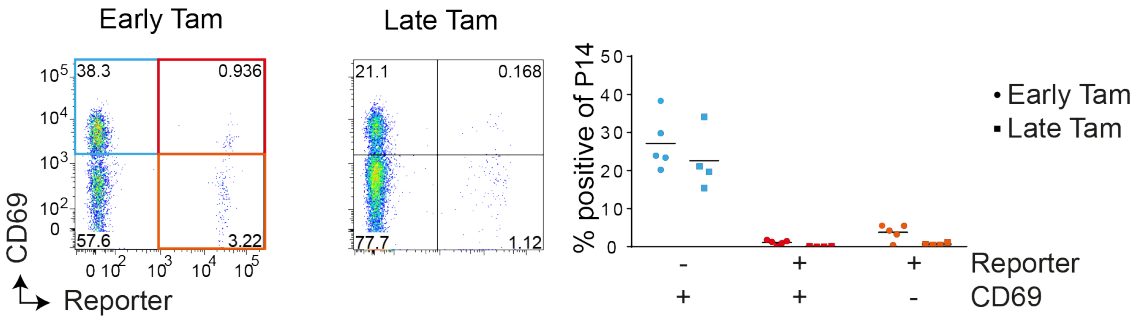

Figure 9: **Reporter construct does not reflect CD69 protein levels during memory phase.** Vb5 mice received 10000 CD69-dTomato-reporter CD45.1^{+} P14 cells and on the same day an i.p. infection with 2x10^{5} pfu LCMV-Arm. The host mice received 100 mg/kg tamoxifen on d0 and d1 or d20 and d21. Shown are representative plots for CD69 and reporter expression and percentages of reporter and/or CD69 positive cells on d28 after infection.

When tamoxifen was administered early on day 0 and 1 a reporter protein expression of about 5 % of all cells was observed (Figure 9). This was substantially higher than the reporter protein expression after late administration of tamoxifen on days 20 and 21, when only about 1 % of the transferred cells expressed the reporter. Furthermore, after late tamoxifen administration, it was expected, that only CD69 expressing cells show reporter expression as only Trm in the tissue express this marker during memory phase. Nevertheless, about half of the reporter positive cells expressed no CD69, which leads to the conclusion, that the surface expression of CD69 and therefore the Trm status of a memory cell cannot be reliably shown with this reporter construct.

3.1.2 DTR rescue strain to delineate Trm function

To gain further insight in the contribution of CD103$^+$ Trm during infection, it is desirable to eliminate all other memory cells before reinfection. Here, a system is validated that leaves only the cell type of interest intact while eliminating all other transgenic cells. The system is based on the constitutive expression of the simian DTR, which renders cells vulnerable to diphtheria toxin. The DTR gene is flanked by loxp sites and can thus be excised by Cre. This transgenic mouse model was crossed to the CD103-zsGreen-reporter model (rescue-CD103-model) to rescue only CD103$^+$ Trm and show their specific influence during reinfection (Figure 10).

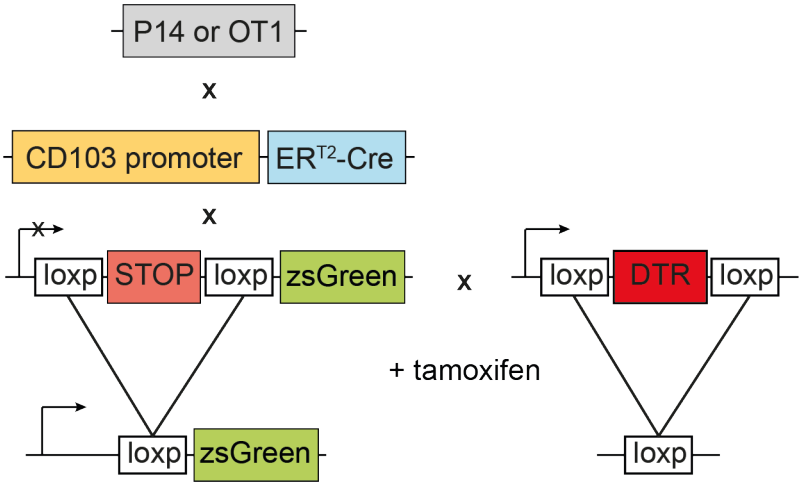

Figure 10: **Graphical illustration of the CD103 based rescue system.** P14 or OT1 mice were crossed to CD103-zsGreen-reporter mice, which carry a CD103 driven ER^{T2}-Cre and a floxed STOP-codon in front of a fluorescent reporter. Further the mice were crossed to mice that carry a floxed DTR. Tamoxifen enables translocation of ER^{T2}-Cre to the nucleus, where it excises a STOP-codon, allowing fluorescent reporter transcription and excision of the DTR. Consequently, these rescue-CD103 model cells are resistant to diphtheria toxin.

To test the efficacy and specificity of the rescue-CD103-model, mice received rescue-CD103-model P14 cells and were infected with LCMV-Arm. During memory phase the mice received tamoxifen twice and were then treated with DTX. Figure 11 shows the efficient deletion of CD103$^-$ cells in the SI and circulating memory cells in the spleen after DTX application. It can also be observed, that the CD103 reporter does not label all CD103$^+$ cells that were rescued from DTX.

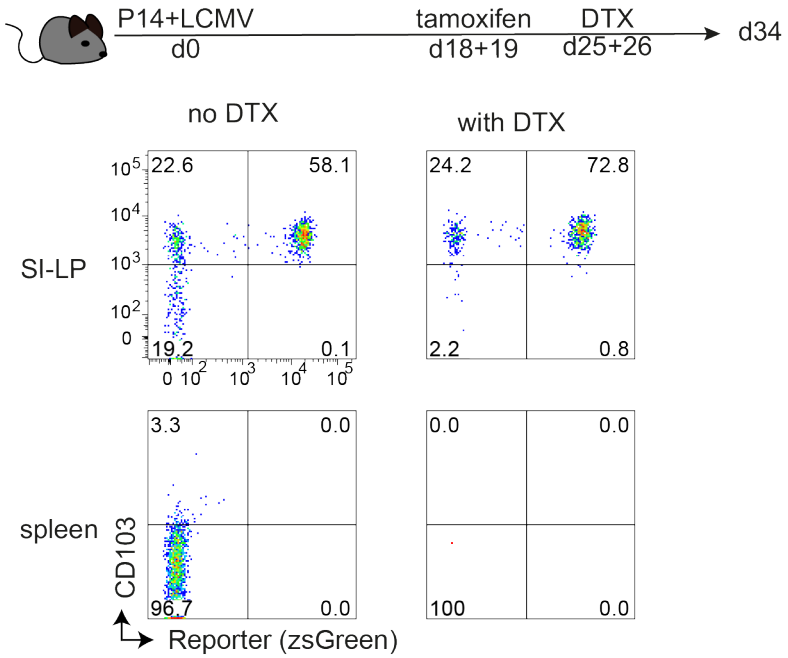

Figure 11: **DTR rescue system specifically protects CD103 expressing cells in the SI-LP.** Mice received 5000 rescue-CD103-model P14 and were infected with $2x10^5$ pfu LCMV-Arm on d0. On d18 and d19 tamoxifen and on d25 and d26 DTX was administered. Representative flow cytometry plots are shown for d34 from spleen and SI-LP for CD103 and reporter expression.

Conclusively, the rescue-CD103-model was shown to precisely eliminate circulating memory and $CD103^-$ Trm cells. Therefore, this can be used in a secondary infection to investigate the specific contribution of $CD103^+$ Trm during rechallenge.

3.1.3 Quantitative fluorescence imaging of local immunity

Imaging can yield valuable insight into biological processes, as it combines location with phenotypical information of cells within tissues. The challenge is the generation of quantitative data from images that substantiate the qualitative impression of human interpretation of imaging data. Thus, un unbiased approach to localize cells and determine organ structures is needed to test hypotheses about cell location and function.

Therefore, several image segmentation methods have been developed earlier that range from manual localization of cells, user specific pipelines, that depend on features and image transformation, and deep learning (Berg et al. 2019; Stringer et al. 2020; McQuin et al. 2018). All these methods aim to separate background from signal, for example cells within organs. The difficulty to achieve this aim increases with cells or structures, that are not separated well from each other or that show only weak signals. Here, user specific pipelines were developed for single cell or organ structure detection in vivo as well as cell detection in vitro. The definition of cells and structures in organs or in vitro enabled to address scientific questions that can be answered in an unbiased, efficient, and reproducible way. Generally, the cells and structures were vectorized by image segmentation, which enabled quantitative analysis of the images.

3.1.3.1 Basic workflow of analysis

For qualitative image analysis a generalized workflow was developed, that can be applied to different biological settings. Figure 12 shows an example for the vectorization of a spleen section. Structures like T – and B cell zones are vectorized, as well as single cells like dendritic cells and T cells.

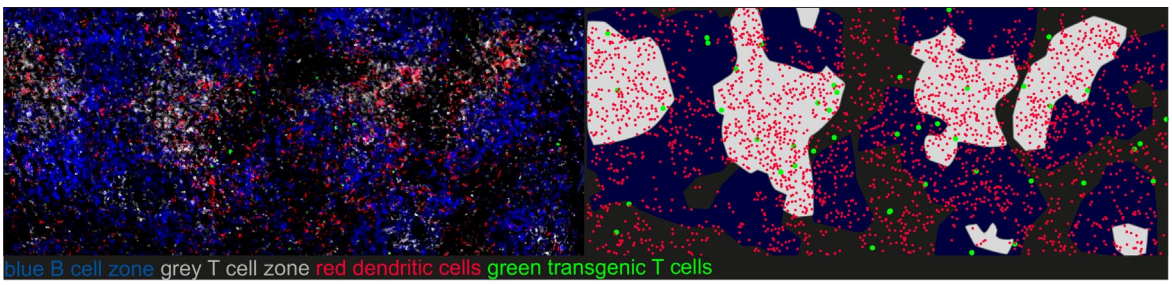

Figure 12: **Vectorization of an immunofluorescent image of a spleen section**. Mice received LCMV-specific P14 cells and were infected with LCMV-Arm. 30 days later, spleens were harvested and stained. Spleen structures B cell zone and T cell zone are shown in blue

and grey, respectively. Dendritic cells are shown in red and transgenic T cells in green. On the left the composite immunofluorescent image is shown, on the right the vectorized version is depicted.

To achieve this visualization and generate a basis for calculations the workflow shown in figure 13 was used.

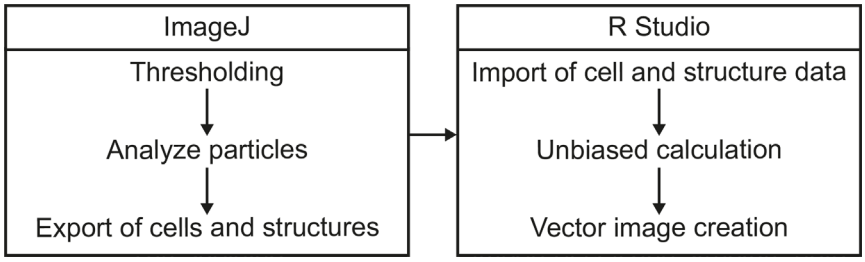

Figure 13: **General workflow for biological imaging data analysis.** First ImageJ was used to identify cells and structures in images and then R was applied to perform calculation and vectorization.

Basically, the program ImageJ is applied to preprocess the image to produce a binary image that only contained information about signal versus background. This results in an image, which contains two colors. Hence, the image is separated in pixels that show signal, for example cells and pixels that show background. To extract the position of the cells or structures out of the pixel image, the tool “Analyze particles” from ImageJ is applied. This enables the extraction of the coordinates of pixel-based particles, according to their size and shape. The extracted cells and structures are then exported to be further processed in R Studio. There, the coordinates are imported and vectorized to enable unbiased calculations with the data and the creation of the vectorized image.

3.1.3.2 Examples of applications for vectorized image analysis

The main goal of vectorization of biological images is the unbiased analysis of these images. The developed unbiased quantitative analysis algorithm was already applied in a range of applications, as imaging data contains valuable information about the location of a cell in relation to other cells and within organs.

The algorithm was used to show an attraction of natural killer cells (NK cells) by neurons in the white pulp of the spleen during infection, by the reduction of distance between the two cell types (Diaz-Salazar et al. 2020).

Further, the localization of a cell within the organ and its substructures can give valuable insights about their function, activation status or interaction with other cell types. Thus, the vectorization algorithm was applied to find the zonal location Tox deficient $CD8^+$ T cells. Thereby, splenic zones like the B cell zone and the T cell zone and T cells were immunofluorescently labeled and vectorized. This enabled the calculation of the distribution of the T cells in the different zones of the spleen and showed that the location of the T cells without Tox showed no different migration pattern (Alfei et al. 2019).

The algorithm can also be used in vitro. When CD8 T cells are activated in vitro, they form proliferative clusters. These clusters can be imaged by brightfield microscopy, and their size can be calculated. This was performed to assess the different potential to respond to IL-2 by CD8 T cells derived from mice that lack PTPN2 or wild type mice (Flosbach et al. 2020).

A detailed analysis of Trm in different tissues and their relationship with other cell types lies outside the scope of this work but can be achieved with the method shown above.

3.2 CD103-fate-mapping characterizes resident cell population

The exact behavior of Trm during reinfection has not been easy to understand because Trm in tissues could not be distinguished with certainty from immigrating circulating cells. Since the newly developed CD103 driven fate-mapping model has proven to be reliable, it is now used here to learn more about the behavior of Trm during reinfection. Thereby, a CD103$^+$ Trm population is described, that exhibits minimal expansion capacity and is phenotypically and locally stable. During secondary infection, the CD103$^+$ Trm compartment is numerically shifted towards reporter$^-$ Trm, which implies a replacement of preexisting CD103$^+$ Trm during rechallenge. Gene expression analysis revealed a response potential of CD103$^+$ Trm to inflammation that is potentiated by antigen presentation.

The following analysis of CD103$^+$ Trm describes these novel insights, that could only be achieved by the highly specific and inducible CD103 driven fate-mapping model.

3.2.1 CD103$^+$ Trm show no reexpansion and are replaced

The expression of adhesion and activation molecules, that often overlap with Trm markers like CD103 makes it hard to determine the fate of Trm during reinfection, as newly arriving cells show the same phenotype as established Trm. With the CD103-zsGreen-reporter model it is possible to specifically label Trm during memory phase and track them during reinfection by their stable expression of the reporter molecule.

Therefore, CD103-zsGreen-reporter-OT1 cells were transferred into Bl6 hosts and infected with Lm-OVA. During memory phase the mice received tamoxifen to activate reporter expression and were reinfected shortly after with VSV-OVA. Figure 14 shows the kinetic of reporter$^+$ Trm and all OT1 cells over the course of infection.

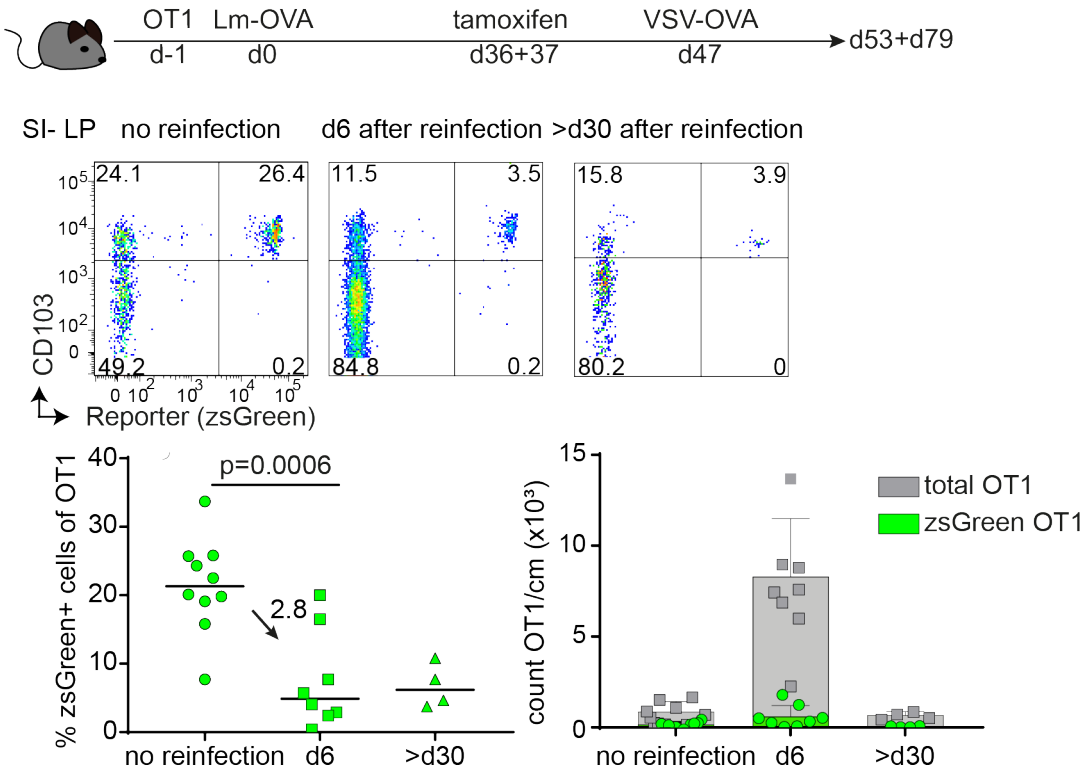

Figure 14: **Reporter⁺ Trm show low expansion potential during reinfection.** Bl6 mice received 5000 CD103-zsGreen-reporter-OT1 on d-1 and were infected on d0 with 1000 cfu Lm-OVA. On d36 and d37 mice received 100mg/kg tamoxifen and were rechallenged with $2x10^6$ pfu VSV-OVA on d47. Shown are representative flow cytometry plots for CD103 and reporter zsGreen expression, frequency of zsGreen⁺ CD103-zsGreen-reporter-OT1 and absolute numbers of zsGreen⁺ CD103-zsGreen-reporter-OT1 and total CD103-zsGreen-reporter-OT1 on d53 and d79 from SI-LP. Unpaired t-test was performed.

During reinfection, the frequency of the reporter⁺ Trm decreased, while an increase in total OT1 cells can be observed (Figure 14). On day 6 the majority of OT1 cells in the SI-LP are CD103⁻ cells, which either leave the tissue after the infection is resolved or die, as they cannot be found in great numbers on >d30 after reinfection. This shows that the CD103⁺ Trm only expand to a small extent by absolute numbers and become a minority in the cell pool during reinfection. The cells cannot resume their frequency from before reinfection at later time points, as their frequency stays about 2.8 times lower than before reinfection. Further, the frequency of the reporter⁺ Trm within the CD103⁺ T cell pool was assessed (Figure 15).

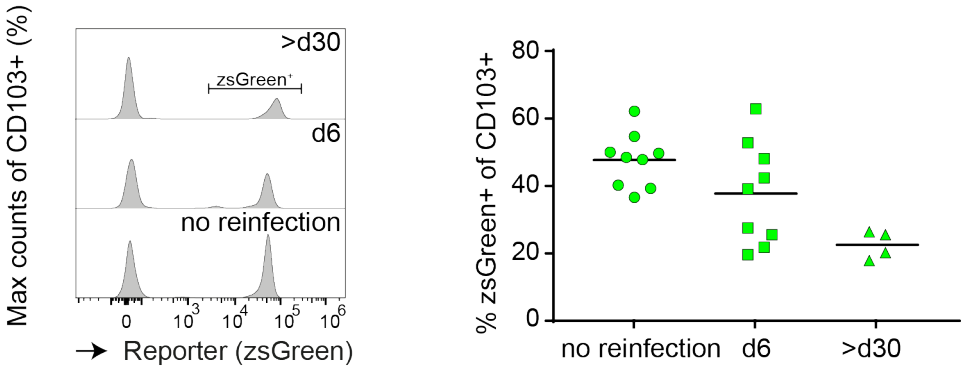

Figure 15: **Reporter$^+$ Trm are replaced during reinfection by CD103$^+$ cells.** Bl6 mice received 5000 CD103-zsGreen-reporter-OT1 on d-1 and were infected on d0 with 1000 cfu Lm-OVA. On d36 and d37 mice received 100mg/kg tamoxifen and were rechallenged with $2x10^6$ pfu VSV-OVA on d47. Shown are representative histograms for reporter expression of CD103$^+$ OT1 and the frequency of zsGreen$^+$ CD103-zsGreen-reporter-OT1 of all CD103$^+$ CD103-zsGreen-reporter-OT1 on d53 and d79 from SI-LP.

This showed the replacement of originally installed reporter$^+$ Trm during reinfection by newly established CD103$^+$ Trm, as the frequency of zsGreen$^+$ Trm declined during and after reinfection.

As reporter$^+$ Trm did not expand and were replaced, the phenotype of the OT1 cells in the SI-LP was analyzed to compare their phenotype to Tem, which generally also show no expansion potential (Figure 16).

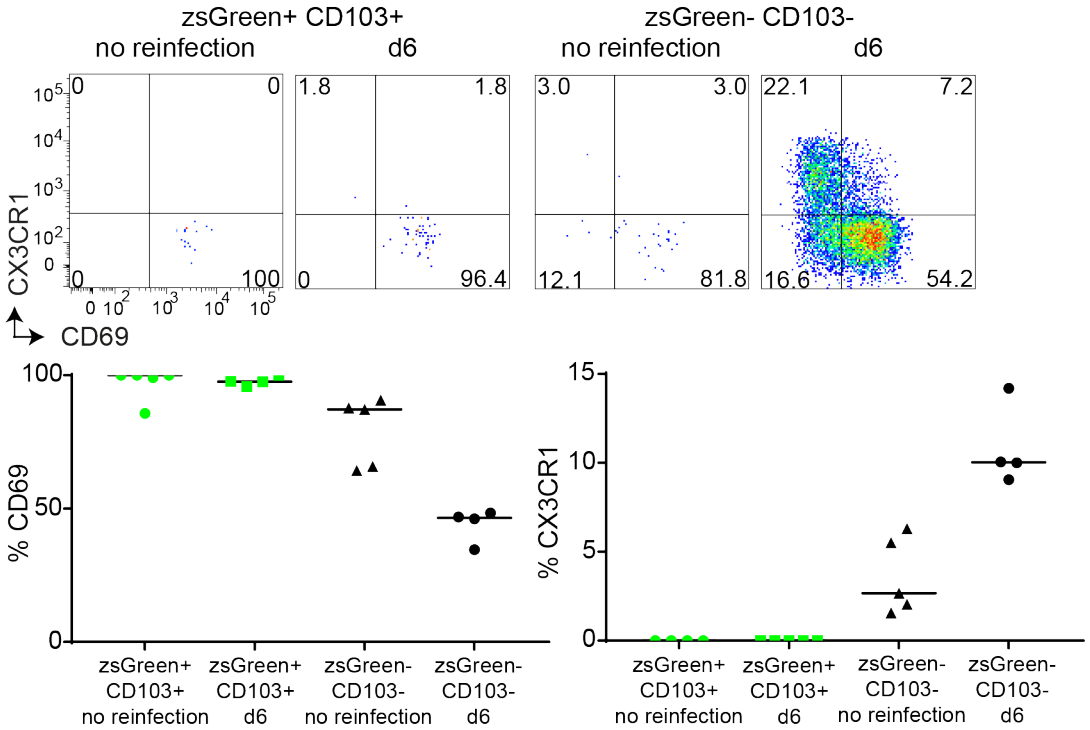

Figure 16: **Reporter⁺ Trm show a stable phenotype.** Bl6 mice received 5000 CD103-zsGreen-reporter-OT1 on d-1 and were infected on d0 with 1000 cfu Lm-OVA. On d36 and d37 mice received 100mg/kg tamoxifen and were rechallenged with $2x10^6$ pfu VSV-OVA on d47. Shown are representative flow cytometry plots for CX3CR1 and CD69 expression of zsGreen⁺CD103⁺ or zsGreen⁻CD103⁻ CD103-zsGreen-reporter-OT1 on d6 after reinfection or without reinfection. Further the frequencies for CD69 and CX3CR1 of zsGreen⁺CD103⁺ or zsGreen⁻CD103⁻ CD103-zsGreen-reporter-OT1 are shown on d6 after reinfection or without reinfection. All data are derived from the SI-LP.

Reporter⁺ Trm and zsGreen⁻CD103⁻ OT1 cells in the SI-LP show a classical Trm phenotype with a high CD69 expression during steady state (Figure 16). After reinfection, the reporter⁺ Trm remain CD69 high and show no upregulation of CX3CR1. ZsGreen⁻CD103⁻ cells, in contrast, show an increase in CX3CR1 expression. This could be due to differentiation of these cells or influx of Tem cells with a CD103⁻ phenotype. Yet, reporter⁺ Trm do not acquire a Tem phenotype and stay phenotypically stable during reinfection.

This led to the question if there was local antigen presentation in the SI-LP because the low proliferation of the reporter⁺ cells could also be attributed to lacking antigen recognition. To test this, Nur77-reporter cells, which express GFP upon TCR activation were employed. Since Nur77-P14 mice were available, the infection sequence was altered to Lm-gp33 primary and LCMV as a secondary infection. The different infection

system was first validated to show the same decrease of frequency among antigen specific T cells in the SI-LP on day 6 after reinfection (Figure 17).

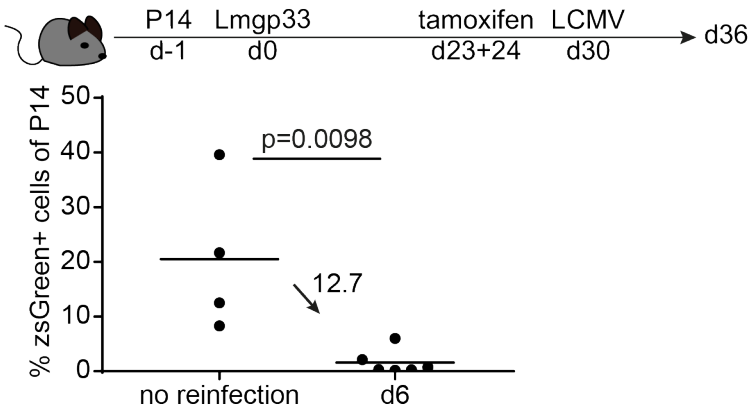

Figure 17: **P14 based reinfection system recapitulates decrease in frequency after reinfection.** Bl6 mice received 10000 CD103-zsGreen-reporter-P14 cells on d-1 and were infected with 1000 cfu Lm-gp33 on d0. On d23 and d24 100mg/kg tamoxifen was administered and on d30 mice were infected with $2x10^5$ pfu LCMV-Arm. Shown is the frequency of $zsGreen^+$ cells of CD103-zsGreen-reporter-P14 on d6 after reinfection. Unpaired t-test was performed.

After the confirmation of the decreased frequency of $reporter^+$ Trm after reinfection, a Nur77-P14 experiment was set up. Mice received Nur77-P14 cells and were infected with Lm-gp33. During memory phase mice were rechallenged with LCMV-Arm and the fluorescence intensity of Nur77 was assessed 24h, 48h and 72h after reinfection (Figure 18).

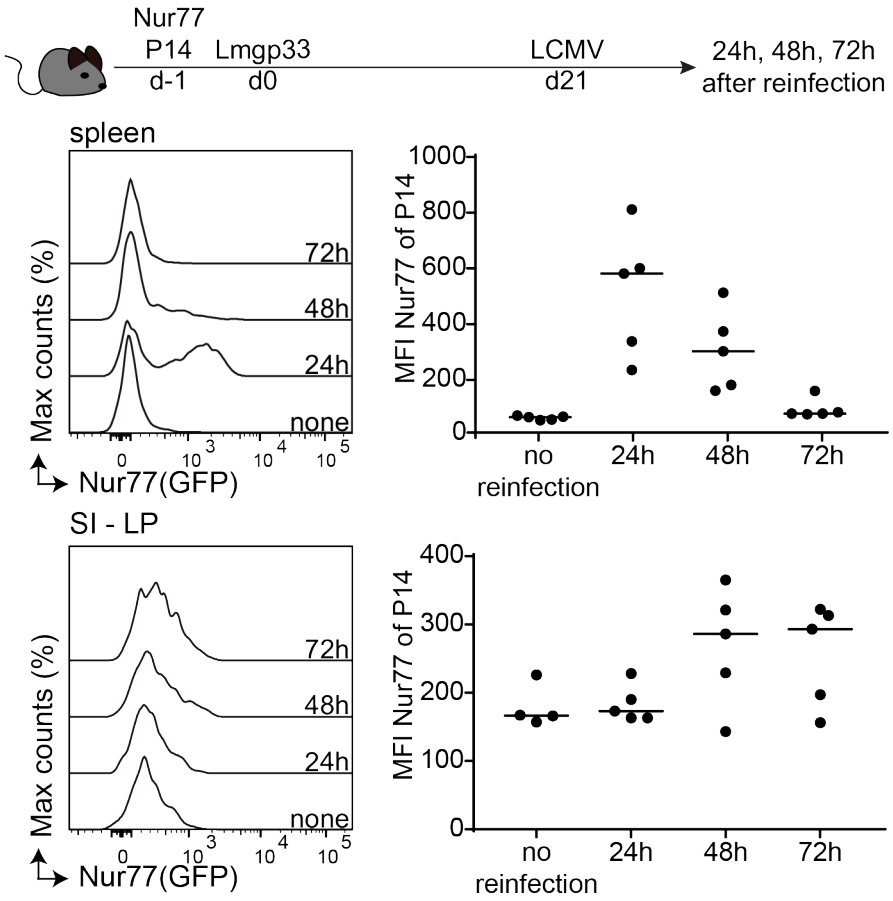

Figure 18: **Nur77 expression in the SI-LP shows antigen recognition in the organ.** Bl6 mice received 10000 Nur77-P14 cells on d-1 and were infected with 1000 cfu Lm-gp33 on d0. On d21 mice were infected with $2x10^5$ pfu LCMV-Arm and the expression of Nur77 was assessed 24 h, 48 h, 72 h and without reinfection. Shown are representative histograms and the mean fluorescence intensity of Nur77 of P14.

Nur77 expression could be detected earlier and stronger in the spleen than in the SI-LP. Nevertheless, higher Nur77 expression could be observed at 48h and 72h after reinfection in the SI-LP. This leads to the conclusion that antigen can be recognized in the SI-LP in the used infection setups.

As Trm are usually found at barrier tissues and act as one of the first cell types that encounter pathogens during rechallenge, the infection route could make a difference in their behavior and especially their proliferation. Therefore, the infection setups of Lm-OVA+VSV-OVA or Lm-gp33+LCMV-Arm, which establish systemic rechallenges, were extended by a local reinfection setup. Mice received a transfer of CD103-zsGreen-reporter-OT1 cells and were primarily infected with VSV-OVA. During memory phase they received tamoxifen and were then rechallenged with an InternalinA (InlA) mutated strain of Lm-OVA (Lm-OVA-Ina_mut) by oral gavage. Wild-

type Listeria have an impaired ability to enter murine intestinal epithelial cells as the binding molecule E-cadherin on the surface of the murine cells has an amino acid change that prevents the binding of the virulence factor InlA. Therefore, the new strain Lm-OVA-Ina_mut was generated by conjugation of a Lm-OVA strain with E.coli carrying the ppL2 plasmid containing a murinised version of InlA (data not shown). Figure 19 shows a 2.4-fold decrease in the percentage of reporter$^+$ Trm and an increase in the general OT1 cell number on day 6 after oral reinfection.

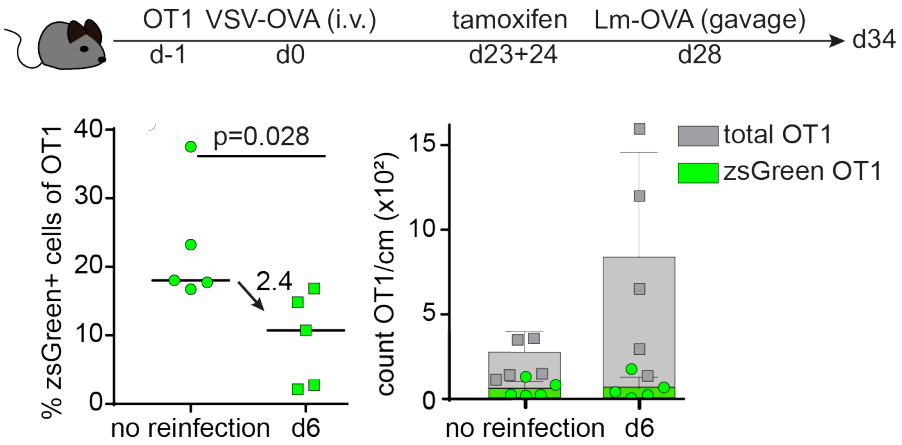

Figure 19: **Oral rechallenge confirms stable phenotype during rechallenge**. Bl6 mice received 5000 CD103-zsGreen-reporter-OT1 cells and were infected with 2x10^6 pfu VSV-OVA on d0. On d23 and d24 mice received 100 mg/kg tamoxifen and were reinfected on d28 with 10^9 cfu Lm-OVA-Ina_mut via oral gavage. The graphs show the percentage of zsGreen$^+$ CD103-zsGreen-reporter-OT1 cells and the count of total and zsGreen$^+$ CD103-zsGreen-reporter-OT1 on d6 after reinfection and without reinfection. Unpaired t-test was performed.

These findings are in line with the systemic rechallenge data in figure 16, which also showed a decline in reporter$^+$ Trm percentages and an increase in the OT1 population.

Thus, reporter$^+$ Trm show a low expansion potential in both systemic and local rechallenge and are replaced during reinfection by newly arriving cells.

3.2.2 CD103⁺ Trm do not leave their organs

Trm have been traditionally described by their restricted migratory behavior. Nevertheless, recent reports show tissue exit of Trm by restimulation. As it is not clear by the so far presented data if the stable number of reporter⁺ Trm is due to the lack of migration or migration with an in situ division, the question was raised whether CD103⁺ Trm leave their organ after reinfection. To address this question the stable and inducible CD103-zsGreen-reporter model is ideal, as reporter⁺ Trm specifically mark initially resident cells. Therefore, other organs were analyzed before and during reinfection, but only a very small number of reporter⁺ cells could be found in mesenteric lymph nodes (MLN) and spleen (Figure 20). The frequency of OT1 of CD8⁺ T cells in MLN and spleen increased, which confirmed a robust systemic reinfection. Therefore, CD103⁺ Trm were found to be locally restricted and did not leave their organ.

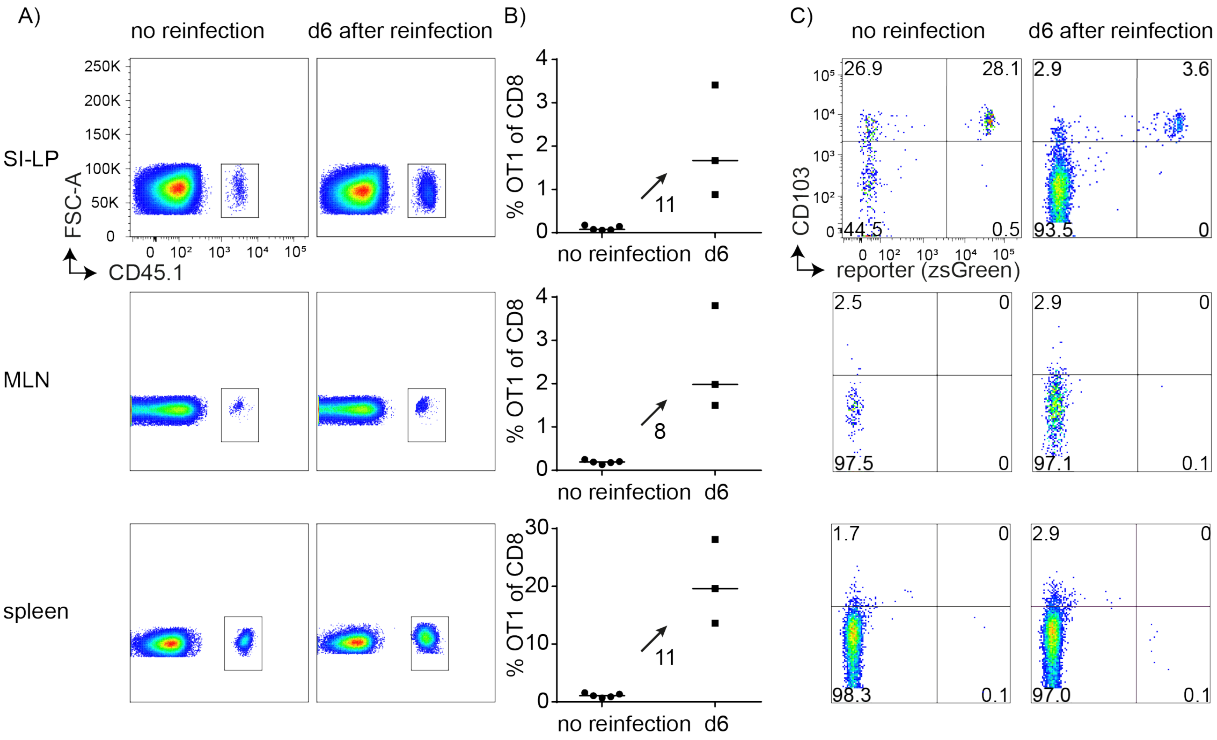

Figure 20: **Reporter⁺ Trm do not leave their organs.** Bl6 mice received 5000 CD103-zsGreen-reporter-OT1 on d-1 and were infected on d0 with 1000 cfu Lm-OVA. On d36 and d37 mice received 100mg/kg tamoxifen and were rechallenged with $2x10^6$ pfu VSV-OVA on d47. Shown are representative flow cytometry plots for CD45.1 and FSC-A to determine CD103-zsGreen-reporter-OT1, and their frequency without reinfection and on d6 after reinfection. Further representative flow cytometry plots are shown for CD103 and reporter expression without reinfection and on d6 after reinfection.

The local stability of the reporter$^+$ Trm during reinfection led to the question if the cells remain at their location in the organ during reinfection or if they change their position. Thus, reporter$^+$ Trm were analyzed in the SI-LP with immunofluorescence microscopy to determine their localization (Figure 21).

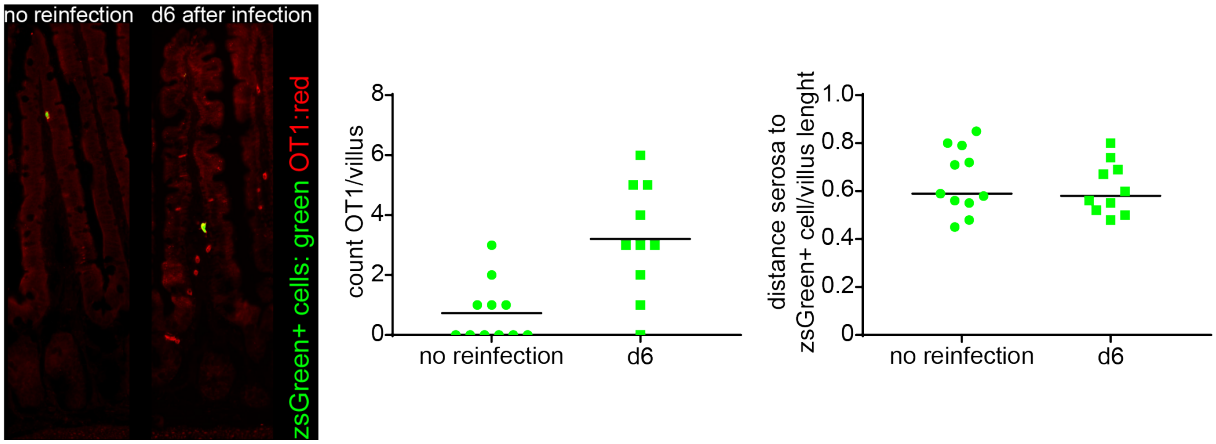

Figure 21: **Reporter$^+$ Trm cells remain in place after reinfection**. Bl6 mice received 5000 CD103-zsGreen-reporter-OT1 on d-1 and were infected on d0 with 1000 cfu Lm-OVA. On d36 and d37 mice received 100mg/kg tamoxifen and were rechallenged with 2x10^6 pfu VSV-OVA on d47. Shown are representative images from d6 after reinfection or without reinfection of the SI. Further the count of CD103-zsGreen-reporter-OT1 per villus and the distance of the serosa to the reporter$^+$ Trm is shown.

Figure 21 shows CD103-zsGreen-reporter cells in the villi during steady state and six days after infection. The reporter$^+$ Trm remained on their position and an increase in total OT1 in the villi could be observed. This further confirmed the local restriction of the reporter$^+$ Trm.

3.2.3 Genetic analysis of Trm reveals antigen specific gene set

To further gain insight in the function of SI-LP lymphocytes separated by CD103 and reporter expression, a bulk NGS analysis was performed. Therefore, Bl6 mice received CD103-zsGreen-reporter-OT1 and were infected with Lm-OVA. After tamoxifen treatment during memory phase the mice were either infected with VSV-OVA (antigen specific restimulation), VSV-wt (antigen unspecific inflammatory

restimulation) or received no reinfection. CD103$^+$zsGreen$^+$, CD103$^+$zsGreen$^-$ and CD103$^-$zsGreen$^-$ cells were sorted from the SI-LP on day 2 after reinfection.

First, the genetic individuality of the 3 sorted populations during steady state and early after reinfection was evaluated by principal component analysis (PCA) (Figure 22A). PCA showed a distinct clustering of the populations from each other by PC2 and a clear distinction of infected and uninfected samples by PC1.

The CD103$^+$zsGreen$^-$ showed only 33 differentially expressed genes from the CD103$^+$zsGreen$^+$ population (data not shown), which underlines the similarity of these populations. Yet, the CD103$^+$zsGreen$^+$ population was clearly distinct from CD103$^-$zsGreen$^-$ during steady-state as 444 genes were differentially expressed (Figure 22B).

During steady-state Ingenuity pathway analysis (IPA) of genes differentially expressed by CD103$^+$zsGreen$^+$ in contrast to CD103$^-$zsGreen$^-$ cells demonstrated that pathways that involve factors that are correlated with decreased TCR sensitivity (IL-10-signaling), innate-like surveillance of pathogens (LPS-signaling), persistence of Trm (4-1BB signaling) and DC-licensing (CD40 signaling) are upregulated in reporter$^+$ Trm in respect to CD103$^-$zsGreen$^-$ cells (Zhou et al. 2019; Meunier et al. 2012; Smith et al. 2018). Genes that were found in the CD103$^-$zsGreen$^-$ cells showed a heterogenous phenotype consisting of Trm markers in combination with markers of circulating memory cells like KLRG1, Eomes, Sell and S1pr1.

Conclusively, the tissue residing subsets consisting of CD103$^+$zsGreen$^+$ cells and CD103$^-$zsGreen$^-$ cells are genetically distinct and an innate like sensor function of reporter$^+$ Trm can be inferred during steady state.

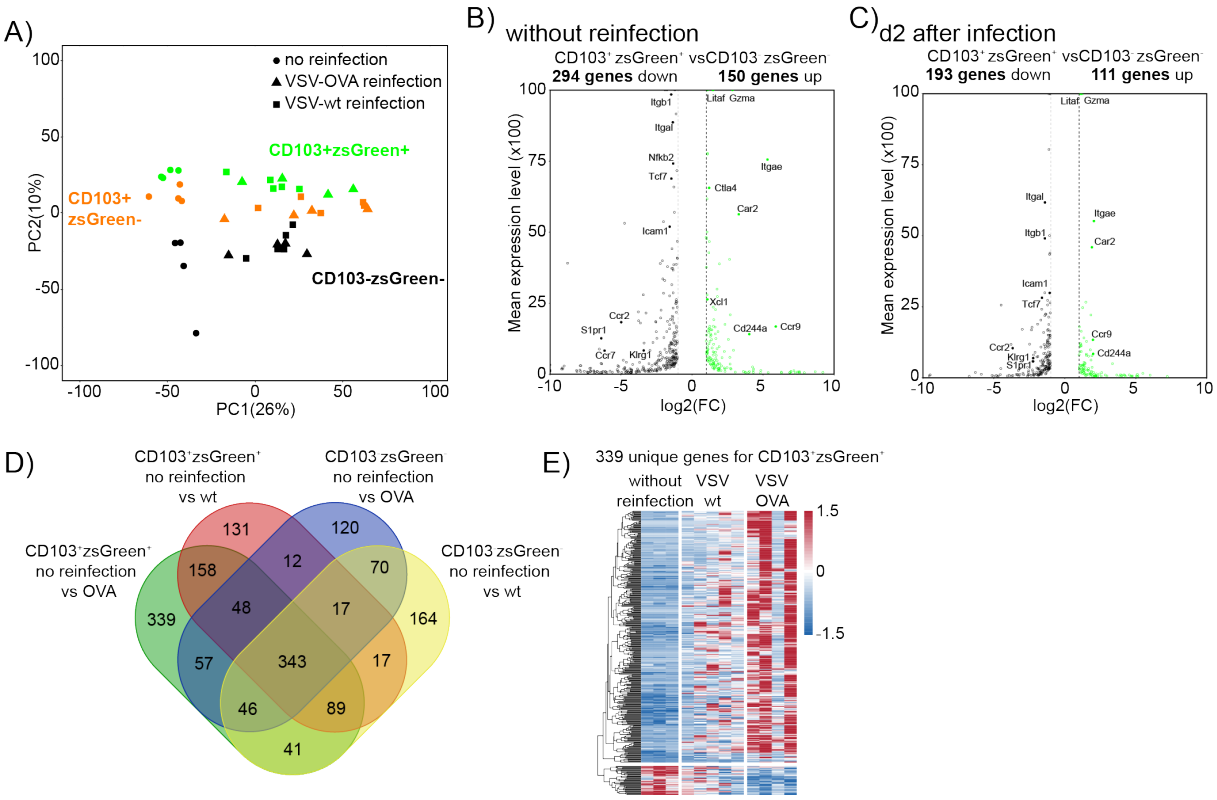

Figure 22: **Genetic analysis reveals antigen specific reactivation of Trm.** Bl6 mice received 10000 CD103-zsGreen-reporter-OT1 and were infected with 1000 cfu Lm-OVA. 100mg/kg tamoxifen was administered on d15 and d16, infection with $2x10^6$ pfu VSV-OVA or VSV-wt occurred on d26. $CD103^+zsGreen^+$, $CD103^+zsGreen^-$ and $CD103^-zsGreen^-$ were sorted from mice that received a reinfection and a control group that received no reinfection. Shown are A) a PCA plot for the 3 sorted cell types on d2 after reinfection or without reinfection. B,C) Volcano-plots depict differentially expressed genes from $CD103^+zsGreen^+$ in relation to $CD103^-zsGreen^-$ cells without reinfection and on d2 after reinfection. D) Venn diagram shows the overlap of differentially expressed genes between no reinfection and reinfection conditions with VSV-OVA and VSV-wt for $CD103^+zsGreen^+$ and $CD103^-zsGreen^-$ cells. D) Heatmap illustrates the 339 unique genes that are differentially regulated in $CD103^+zsGreen^+$ after VSV-OVA reinfection. The differentially expressed genes used to compute the volcano-plot and venn diagram were filtered for mean expression ≥50, adjusted $P \leq 0.05$ and log-foldchange ≥ 1 and ≤ -1.

Next, the question was asked how the $CD103^+zsGreen^+$ cells and $CD103^-zsGreen^-$ cells react early during reinfection. Figure 22C shows a volcano plot with 304 differentially expressed genes between $CD103^+zsGreen^+$ cells and $CD103^-zsGreen^-$ cells on day 2 after reinfection with VSV-OVA. This substantiated the unique identities and differential response of $CD103^+zsGreen^+$ cells and $CD103^-zsGreen^-$ cells to

reinfection. After confirming the uniqueness of the subsets, it was interesting to further delineate which contribution inflammation played in this reaction. Therefore, a comparison of differentially expressed genes of the CD103^{+}zsGreen^{+} subset and CD103^{-}zsGreen^{-} subset before and after reinfection with either VSV-OVA or VSV-wt infection was done. Figure 22C shows a venn diagram that depicts the overlap of genes that are differentially regulated in the different subsets, but also in the antigen specific and unspecific restimulation. For the CD103^{+}zsGreen^{+} population 339 genes were found that were only differentially regulated in this population in the antigen specific VSV-OVA reinfection. Therefore, these genes are the distinct signature of reporter^{+} Trm during antigen specific reinfection. Figure 22D shows a heatmap of these genes. The genes that are upregulated or downregulated differ strongly from the uninfected condition, but the antigen unspecific rechallenge shows a certain degree of activation of those genes. This led to the conclusion, that reporter^{+} Trm are substantially affected by inflammation, but need antigen for a full activation of their recall response. Genes that were specifically upregulated in reporter^{+} Trm during VSV-OVA reinfection included VCAM1, TLR13 and Il22, which were shown to be important in noncytotoxic antiviral response activity, integrity of the intestinal barrier and expression of antimicrobial peptides (Diaz et al. 2005; Moyat et al. 2017). Additionally, genes associated with negative regulation of immune responses were found, like PD-L1 and Il1rl.

In conclusion, reporter^{+} Trm were found to be a distinct Trm subset with unique gene expression during steady state and infection. While their recall response to mere inflammation overlaps with the antigen specific response, they have a unique gene set responding strongly to antigen. This response balances effector function with protection of tissue integrity by inducing an anti-pathogenic state while also upregulating negative regulators of the immune response.

Chapter 4

Discussion

Trm reside in a variety of barrier tissues and are also found e.g.in lymphoid organs (Schenkel et al. 2014b). During rechallenge Trm are important players in local immune defense against invading pathogens, as they can protect the host from pathogen spread and boost sterilizing local immunity. (Schenkel et al. 2014a; Ariotti et al. 2014; Jiang et al. 2012; Schenkel et al. 2013).

It is therefore favorable to gain further insight into the biology of Trm to employ them in knowledge-based interventions to install immune protection, like vaccines. Such vaccines have already shown promising protection and specifically use Trm at entry points of the pathogen in the context of HPV, SIV and Ebola (Çuburu et al. 2012; Hansen et al. 2011; Nizard et al. 2017; Meyer et al. 2015).

To further increase the understanding of how to use the therapeutic potential of Trm, it is vital to deepen the knowledge about their maintenance and function. Especially, how these cells behave over time and during rechallenge leads to insights that can help to develop vaccines that can ensure long-term stability and maximal anti-pathogenic potential of Trm.

Therefore, a faithful fate-mapping model was developed and used to investigate the specific behavior and contribution of Trm during reinfection. Unexpectedly, $CD103^{+}$ Trm were found to have a low reexpansion capacity and were replaced by newly formed Trm. The cells further stayed in the tissue during reinfection and showed an inflammation and an additional antigen specific response to reinfection.

In the following, the results of the CD103 based system will be discussed first. Subsequently, the insights and opportunities of the CD69-based system, which does not report Trm reliably in this specific configuration, will be presented.

4.1 CD103 reporter system reveals CD103$^+$ Trm as local sentinels in tissues

CD103 was chosen as a marker to fate map Trm over long periods of time and study their behavior during reinfection, because it is found on many Trm during steady state (Mackay et al. 2013a). Therefore, transgenic mice carrying a CD103 driven ER^{T2}-Cre were crossed to reporter mice that contain a floxed STOP-codon in front of the fluorescent reporter zsGreen. This resulted in a temporally tightly controlled reporter system for CD103$^+$ Trm.

First the specificity of the CD103-zsGreen-reporter construct was shown. The reporter labels CD103$^+$ cells reliably during steady state of the whole transgenic mouse and after CD103-zsGreen-reporter cell transfer into Bl6 mice. The frequency of reporter expression among CD103$^+$ cells was about 50 % or higher in the SI-LP in adoptive transfer experiments, which was described as a substantially high frequency for ER^{T2}-Cre dependent reporter systems (Donocoff et al. 2020). The infection used to establish Trm had an influence on reporter expression, as for example the prolonged antigen presentation after VSV infection could lead to the observed expression of the reporter in the spleen (Turner et al. 2007). Further, LCMV-A established a generally larger number of CD103$^+$ cells in the SI-LP Trm pool, which led to a high reporter$^+$ frequency. Yet, the installed CD103$^+$ Trm in the SI-LP showed in all infections a classical Trm phenotype and can therefore be used as model for Trm behavior. Consequently, this fate-mapping model is the first to allow specific tracing of CD103$^+$ Trm during reinfection. This enables the investigation of Trm in their natural environment without the need of parabiosis, adoptive transfer of Trm, subset unspecific ablation of memory cells or transplantation (Beura et al. 2018b; Im et al. 2020; Behr et al. 2020; Schenkel et al. 2013; Masopust et al. 2010).

So, as the specificity of the reporter for Trm was confirmed, the CD103-zsGreen-reporter model was employed to study Trm behavior during reinfection. Surprisingly, only minimal expansion of the CD103$^+$ Trm pool was observed in the SI-LP, while the total number of antigen specific memory T cells highly increased. This was shown not only in the systemic ovalbumin-based and gp33-based system, but also in an oral rechallenge system based on ovalbumin. Recent publications showed an increase of total cells in organs during reinfection, which was thought to stem from a general local Trm proliferation and an influx of circulating memory cells (Beura et al. 2018a; Park et al. 2018). In this work it could be demonstrated that the local cell expansion is not due

to the CD103$^+$ Trm but stems from the CD103$^-$ memory compartment. This heterogeneity in the Trm pool could previously not be appreciated, as only this novel CD103-zsGreen-reporter model enables fate-mapping of CD103$^+$ Trm during reinfection.

The continued low frequency of reporter$^+$ Trm long after reinfection can be linked to the accumulation of memory cells that results in an establishment of additional Trm. The origin of these newly formed Trm that replace the original population is still under investigation and this work shows specifically that the source of novel CD103$^+$ Trm are not preexisting CD103$^+$ Trm, but CD103$^-$ memory cells (Beura et al. 2018a; Osborn et al. 2017).

Recently, another reporter model was established that uses the transcription factor Hobit to label Trm, in order to delineate the fate of Trm during reinfection (Behr et al. 2020). This system is non inducible, which means that the cells are not labeled once at a tightly controlled time point but express the reporter each time Hobit is expressed. The Hobit-reporter mouse was used to show that Hobit expressing memory cells accumulate after reactivation in peripheral tissues and are later also found in circulation (Behr et al. 2020). This does not reflect the behavior of the CD103$^+$ Trm that is described here, but rather reflects the heterogenous CD103$^-$ compartment. Further research needs to delineate if the Hobit-reporter model fate maps CD103$^-$ Trm alone or in conjunction with Tem upregulating Hobit during reinfection.

Concludingly, the presented data is in line with recent publications, as an increase in antigen specific memory cells in the organ can be shown. In addition, the presented work highlights the unique behavior of the phenotypically and numerically stable CD103$^+$ Trm subset in the SI in comparison to the CD103$^-$ cell compartment, which replaces CD103$^+$ Trm in the course of infection.

Further, the residency of the CD103$^+$ Trm could be demonstrated during and after reinfection because no reporter positive cells were found in draining lymph nodes or the periphery. This corresponds to recent papers that looked at the residency of memory cells during chronic infection, where in parabiotic experiments little migration of memory cells between mice was shown (Im et al. 2020). Further, photoconverted cells in the skin did not drain to the lymph nodes after rechallenge (Park et al. 2018). Reports that show draining to the lymph node of reactivated “resident” memory cells rely on surface markers like CD69, that is shared by recently activated cells in the periphery (Beura et al. 2018a). The tissue exit described by the Hobit-reporter model,

goes along the same line, as the reporter is not temporally controlled, and reporter expression does not account for a true resident phenotype during rechallenge (Behr et al. 2020). Thus, tissue exit of CD69 single positive cells in tissues cannot be precluded but the system presented here reliably shows that CD103$^+$ Trm were found to be locally retained.

CD103$^+$ Trm showed limited proliferation and no tissue exit, thus their phenotype during rechallenge was further characterized by an RNA-sequencing analysis. Trm have been shown to improve immunity against recurring pathogens, and their effect goes from cell contact mediated killing to a tissue wide initiation of an anti-pathogenic state (Schenkel et al. 2014a; Ariotti et al. 2014). Genetic analyses presented above showed a clear distinction of CD103$^+$ Trm and the CD103$^-$ cell compartment. While the CD103$^-$ population contained markers from different memory subsets, the CD103$^+$ Trm showed markers of conventional residency during steady state.

CD103 was used before to differentiate Trm subsets in the SI-LP after Yersinia infection (Bergsbaken and Bevan 2015). CD103$^-$CD69$^+$ and CD103$^+$CD69$^+$ cells differ in cytokine and chemokine receptors and persist both within the tissue (Bergsbaken et al. 2017). Others used different markers like Blimp, Id3 or NR4A1 as putative Trm subset markers (Omilusik et al. 2019; Kurd et al. 2020; Boddupalli et al. 2016). Together, the idea of a heterogenous Trm compartment in peripheral organs could be substantiated with the presented data, which show a clear distinction of CD103$^+$ and CD103$^-$ Trm.

Analysis with IPA revealed an innate like sensor function for these cells. This alarm inducing function of Trm was also observed by other groups, but the division in labor regarding proliferation and production of specific chemokines or cytokines has not yet been studied in depth (Mackay et al. 2016; Bergsbaken et al. 2017). CD103$^+$ Trm were found to be reactivated in a non-cognate fashion, which was already described and results from a immunological microenvironment created by the innate immune response (Kadoki et al. 2017; Richer et al. 2013; Steinbach et al. 2016; Soudja et al. 2012). Yet, antigen specific rechallenge revealed a sentinel gene signature that balances effector function with the protection of tissue integrity.

Together the genetic analyses confirmed the previous data, that the CD103$^+$ Trm are a distinct population with a balanced function to protect from antigen and persevere the organ during rechallenge.

Concludingly, a tissue specific division of labor was observed with the $CD103^-$ compartment increasing in number and consisting of a heterogenous memory cell pool, while the $CD103^+$ Trm exhibit minimal proliferation capacity, are replaced during rechallenge, do not leave their organ, and serve as sentinels for pathogenic invasion.

A further delineation of the function of $CD103^+$ cells can also be expected, as the presented rescue system, based on a floxed DTR, works in a specific and efficient manner. This rescue-CD103-model can be employed to eliminate all circulating cells and $CD103^-$ cells in the tissue during steady-state. This opens the door to find out more about the contribution of $CD103^+$ Trm during rechallenge.

4.2 CD69 transgenic model cannot be used in this configuration

A BAC-transgenic CD69 reporter mouse was generated and validated for reliable indication of CD69 expression and specifically Trm identity. Therefore, CD69 reporter mice were crossed to mice carrying a floxed STOP codon in front of either YFP or dTomato. Additionally, the mice were crossed to a P14 background to allow the use in the well-studied LCMV based model. The expression of fluorescent reporter protein was low during early and late labelling. Further, late labelling revealed a CD69 independent activation of the reporter. Thus, this specifically generated mouse strain cannot be used reliably for Trm fate mapping.

One pitfall during the generation of these mice was the low yield in transgenic mice. Only one transgenic pub was retrieved after pronuclear injection. As BAC transgene insertion into the genome happens randomly, it cannot be precluded that the insertion site of the transgene in this founder mouse was in a transcriptionally inactive region or at a too low number (Haruyama et al. 2009). This would lead to a positive genotyping result by PCR, which does not predict efficient reporter activation.

Furthermore, it was shown, that CD69 is regulated not only on the transcript level, but also on the protein level (Bai et al. 2007). S1PR1, which is positively transcriptionally regulated by KLF2, was shown to engage in a competitive protein-protein interaction with CD69. KLF2 overexpression led to decrease of surface CD69 levels, while leaving CD69 mRNA levels intact (Bai et al. 2007). This could lead to incorrect interpretation of the reporter expression, which would stay the same as CD69 surface protein decreases with elevated KLF2 expression.

Further, it was shown, that Cre activity has a cytotoxic effect on highly proliferating cells, due to additional genomic instability (Kurachi et al. 2019). This should be taken into consideration, when tamoxifen is administered early during the immune response in vivo or in vitro. Nevertheless, the reporter expression during memory phase was also at low extent. So, the generally low expression of the reporter was more likely to disadvantageous genetic placement of the construct.

Together, the CD69 fate-mapping approach could still hold potential to be used for Trm characterization. Therefore, new founder mice should be generated and validated for efficacy and specificity. This could be done in a new round of pronuclear injection of the existing BAC or a CRISPR/Cas-mediated knock-in of the ER^{T2}-Cre into the CD69 locus. Further, as the definition of diverse Trm subsets is also dependent on other fate-

mapping markers it could be favorable to generate reporter mice based on different recombinases like flipase to enable combining fate-mapping systems.

Chapter 5

Conclusion and Outlook

Trm remain in peripheral organs and lymphoid tissues after infection and generate local immune responses against re-emerging pathogens. Despite recent insights into their phenotypic properties and site specificity, there are still major uncertainties about their exact behavior upon reinfection. Particularly, since no reliable and unambiguous fate-mapping systems are available that allow Trm-specific cell tracing. Therefore, a reliable fate-mapping model and a complementary system that specifically installs Trm before reinfections was developed in this work to specifically describe the behavior and contribution of Trm during reinfection. These novel models overcome issues of traditional methods for studying Trm, like parabiosis, transplantation or adoptive transfer of memory cells, by allowing Trm to be analyzed in their natural environment without major experimental intervention.

While the CD69-reporter was not reliable to fate map Trm, the CD103-reporter could be used to gain insight in Trm biology. The work demonstrated a specialized $CD103^+$ Trm population in the SI-LP, which has limited reexpansion potential, is replaced with newly formed Trm, and protects in a balanced way between anti-pathogenic interventions and tissue integrity.

Further genetic and functional analysis on these cells could provide more mechanistic insights about their biology. This can be done by expanding the NGS analyses to more timepoints and the use of the rescue-CD103-model, which could specify the protective capacity of this memory cell subset. Further, the quantitative imaging approach can be employed to describe cells in proximity to Trm in tissues and provide more insight into their behavior by statistically analyzing tissue distribution.

$CD103^+$reporter$^+$ Trm are also found during chronic infection (data not shown), and the significance of Trm in chronic infection is still facing large gaps (Im et al. 2020). Therefore, the reporter system should be used in a chronic model to characterize Trm,

especially as their significance in tumors is already established (Webb et al. 2015; Wang et al. 2015).

Further the CD103-zsGreen-reporter can not only be employed in a $CD8^+$ T cell specific way but can also be crossed to other T cell transgenic backgrounds, like CD4 transgenic SMARTA mice (Kilshaw and Murant 1990; Cerf-Bensussan et al. 1987; Oxenius et al. 1998).

Together, the presented CD103-fate-mapping model holds great potential to find out more about the biology of not only Trm but all CD103 expressing cells.

Chapter 6

Materials and Abbreviations

6.1 Materials

Table 1 shows the buffers used for processing of cells and table 2 commercial reagents and kits. Table 3 shows the used antibodies.

Table 1: Solutions for cell processing

Buffer	Composition
FACS buffer	PBS 2% Heat inactivated FCS 0.01% NaN_3
cleaning buffer for SI	PBS 1 % EDTA
digestion solution for SI	RPMI-1640 Medium 2 % HEPES 24 % Liberase TL 1.7 % DNAse
Fixation-buffer	10 ml FACS buffer 2 % formaldehyde
Permeabilization-buffer	0.25 % saponin 0.25 % BSA
ACK-buffer (1x)	0.15 M NH4Cl 1 mM KHCO3 0.1 mM Na2EDTA in dH2O (pH 7.2-7.4)
Medium supplement	5 mM Hepes,

	50 µM 2-Mercaptoethanol, 100 U/ml Penicillin/ Streptomycin

Table 2: Commercial reagents and kits

Reagent	Manufacturer	Cat#
PBS	Sigma-Aldrich, St. Louis, USA	D8537-1L
10 x PBS	Thermo Fisher Scientific, Waltham, USA	10722497
RPMI-1640	Sigma-Aldrich, St. Louis, USA	R8758
BHI	Sigma-Aldrich, St. Louis, USA	53286
Percoll	Cytiva, Bronshoj, Denmark	17-0891-02
Formaldehyde	Sigma-Aldrich, St. Louis, USA	F8775-25ML
Corn oil	Sigma-Aldrich, St. Louis, USA	C8267
Acetone	VWR, Radnor, Pennsylvania, USA	APC131007.1214
Dynabeads Mouse T-Activator CD3/CD28	Thermo Fisher Scientific, Waltham, USA	11453D
(Z)-4-Hydroxy-Tamoxifen	Sigma-Aldrich, St. Louis, USA	H7904-5MG
Tamoxifen	Sigma-Aldrich, St. Louis, USA	10540-29-1
Recombinant hTGF-β1	BioLegend, San Diego, USA	580704
Recombinant mouse IL-2	Peprotech, Hamburg, Germany	212-12
Brefeldin A	Sigma-Aldrich, St. Louis, USA	B7651

DTX	Sigma-Aldrich, St. Louis, USA	322326
Albumin Fraction V	Carl Roth GmbH + Co. KG, Karlsruhe, Germany	2923225
Heparin	VWR, Radnor, Pennsylvania, USA	A3004,0001
EDTA	Sigma-Aldrich, St. Louis, USA	EDS-100G
Agar	Merck, Darmstadt, Germany	1.01615.1000
Heat inactivated FCS	BioCat GmbH, Heidelberg	EXO-FBS-50A-1
CD8a+ T Cell Isolation Kit, mouse	Miltenyi Biotec, Bergisch Gladbach, Germany	130-104-075
Avidin/Biotin Blocking System	BioRad Laboratories Inc, Hercules, Kalifornien, Vereinigte Staaten	BUF016
Prolong Gold mounting buffer	Thermo Fisher Scientific, Waltham, USA	11559306
Zombie NIR™ Fixable Viability Kit	BioLegend, San Diego, USA	423105
Agencourt RNAdvance Cell v.2 kit	Beckman Coulter, Pasadena, USA	A47942
SMART-Seq v.4 Ultra Low Input RNA Kit for Sequencing	Takara/Clontech, Mountain View, USA	634891
Illumina Nextera XT DNA Library reagents	Illumina, San Diego, USA	FC-131-1024
Agilent High Sensitivity DNA Kit	Agilent, Santa Clara, USA	5067-4626
KAPA SYBR FAST qPCR Master Mix	Kapa Biosystems, Wilmington, USA	KK4600

Table 3: Antibodies

Name	Clone	Manufacturer
CXRCR1 PB	SA011F11	Biolegend
CD45.1 PeCy7	A20	eBioscience
CD45.1 eF450	A20	eBioscience
CD69 PE	H1.2F3	eBioscience
CD69 FITC	H1.2F3	eBioscience
CD8 AF700	53-6.7	eBioscience
CD8 BV711	53-6.7	eBioscience
CD103 AF647	2EF	BioLegend
CD62L PeCy7	MEL-14	eBioscience

6.2 Abbreviations

ActA	actin assembly-inducing protein
APC	antigen presenting cells
BAC	bacterial artificial chromosome
cfu	colony forming units
DCs	dendritic cells
DTR	Diphtheria toxin receptor
DTX	Diphtheria toxin
FRT	female reproductive tract
HSV	herpes simplex virus
InlA	InternalinA
i.p.	intraperitoneal injection
IPA	Ingenuity pathway analysis
LCMV	lymphocytic choriomeningitis virus
LCMV-Arm	LCMV-Armstrong
LCMV-c13	LCMV-clone13
Lm	*Listeria monocytogenes*
Lm-OVA-Ina_mut	Listeria monocytogenes with a mutated InternalinA
MZ	marginal zones
MLN	mesenteric lymph nodes
min	minute
NK cell	natural killer cell
OHT	4-hydroxytamoxifen
pfu	plaque forming units
PCA	principal component analysis
RT	room temperature
SI-LP	small intestine lamina propria
TCF1	transcriptional regulator T cell factor 1
Tcm	Central memory T cells
Tem	Effector memory T cells
Tregs	regulatory T cells
Trm	resident memory $CD8^+$ T cells
VSV-OVA	vesicular stomatitis virus-ovalbumin
WP	white pulp

Publication bibliography

Ahmed, R.; Oldstone, M. B. (1988): Organ-specific selection of viral variants during chronic infection. In *J Exp Med* 167 (5), pp. 1719–1724. DOI: 10.1084/jem.167.5.1719.

Alfei, Francesca; Kanev, Kristiyan; Hofmann, Maike; Wu, Ming; Ghoneim, Hazem E.; Roelli, Patrick et al. (2019): TOX reinforces the phenotype and longevity of exhausted T cells in chronic viral infection. In *Nature* 571 (7764), pp. 265–269. DOI: 10.1038/s41586-019-1326-9.

Ariotti, Silvia; Hogenbirk, Marc A.; Dijkgraaf, Feline E.; Visser, Lindy L.; Hoekstra, Mirjam E.; Song, Ji-Ying et al. (2014): T cell memory. Skin-resident memory $CD8^+$ T cells trigger a state of tissue-wide pathogen alert. In *Science (New York, N.Y.)* 346 (6205), pp. 101–105. DOI: 10.1126/science.1254803.

Bai, Ailin; Hu, Hui; Yeung, Mandy; Chen, Jianzhu (2007): Kruppel-like factor 2 controls T cell trafficking by activating L-selectin (CD62L) and sphingosine-1-phosphate receptor 1 transcription. In *Journal of immunology (Baltimore, Md. : 1950)* 178 (12), pp. 7632–7639. DOI: 10.4049/jimmunol.178.12.7632.

Behr, Felix M.; Parga-Vidal, Loreto; Kragten, Natasja A. M.; van Dam, Teunis J. P.; Wesselink, Thomas H.; Sheridan, Brian S. et al. (2020): Tissue-resident memory CD8+ T cells shape local and systemic secondary T cell responses. In *Nat Immunol* 21 (9), pp. 1070–1081. DOI: 10.1038/s41590-020-0723-4.

Bennett, S. R.; Carbone, F. R.; Karamalis, F.; Flavell, R. A.; Miller, J. F.; Heath, W. R. (1998): Help for cytotoxic-T-cell responses is mediated by CD40 signalling. In *Nature* 393 (6684), pp. 478–480. DOI: 10.1038/30996.

Berg, Stuart; Kutra, Dominik; Kroeger, Thorben; Straehle, Christoph N.; Kausler, Bernhard X.; Haubold, Carsten et al. (2019): ilastik: interactive machine learning for (bio)image analysis. In *Nature methods* 16 (12), pp. 1226–1232. DOI: 10.1083/jcb.201004104.

Bergmann, Silke; Beard, Philippa M.; Pasche, Bastian; Lienenklaus, Stefan; Weiss, Siegfried; Gahan, Cormac G. M. et al. (2013): Influence of internalin A murinisation on host resistance to orally acquired listeriosis in mice. In *BMC microbiology* 13, p. 90. DOI: 10.1186/1471-2180-13-90.

Bergsbaken, Tessa; Bevan, Michael J. (2015): Proinflammatory microenvironments within the intestine regulate the differentiation of tissue-resident $CD8^+$ T cells responding to infection. In *Nature immunology* 16 (4), pp. 406–414. DOI: 10.1038/ni.3108.

Bergsbaken, Tessa; Bevan, Michael J.; Fink, Pamela J. (2017): Local Inflammatory Cues Regulate Differentiation and Persistence of CD8(+) Tissue-Resident Memory T Cells. In *Cell reports* 19 (1), pp. 114–124. DOI: 10.1016/j.celrep.2017.03.031.

Bergthaler, Andreas; Flatz, Lukas; Hegazy, Ahmed N.; Johnson, Susan; Horvath, Edit; Löhning, Max; Pinschewer, Daniel D. (2010): Viral replicative capacity is the primary determinant of lymphocytic choriomeningitis virus persistence and immunosuppression. In *Proceedings of the National Academy of Sciences of the United States of America* 107 (50), pp. 21641–21646. DOI: 10.1073/pnas.1011998107.

Beura, Lalit K.; Anderson, Kristin G.; Schenkel, Jason M.; Locquiao, Jeremiah J.; Fraser, Kathryn A.; Vezys, Vaiva et al. (2015): Lymphocytic choriomeningitis virus persistence promotes effector-like memory differentiation and enhances mucosal T cell distribution. In *Journal of leukocyte biology* 97 (2), pp. 217–225. DOI: 10.1189/jlb.1HI0314-154R.

Beura, Lalit K.; Fares-Frederickson, Nancy J.; Steinert, Elizabeth M.; Scott, Milcah C.; Thompson, Emily A.; Fraser, Kathryn A. et al. (2019): CD4+ resident memory T cells dominate immunosurveillance and orchestrate local recall responses. In *The Journal of experimental medicine* 216 (5), pp. 1214–1229. DOI: 10.1084/jem.20181365.

Beura, Lalit K.; Mitchell, Jason S.; Thompson, Emily A.; Schenkel, Jason M.; Mohammed, Javed; Wijeyesinghe, Sathi et al. (2018a): Intravital mucosal imaging of CD8+ resident memory T cells shows tissue-autonomous recall responses that amplify secondary memory. In *Nature immunology* 19 (2), pp. 173–182. DOI: 10.1038/s41590-017-0029-3.

Beura, Lalit K.; Wijeyesinghe, Sathi; Thompson, Emily A.; Macchietto, Marissa G.; Rosato, Pamela C.; Pierson, Mark J. et al. (2018b): T Cells in Nonlymphoid Tissues Give Rise to Lymph-Node-Resident Memory T Cells. In *Immunity* 48 (2), 327-338.e5. DOI: 10.1016/j.immuni.2018.01.015.

Bhardwaj, V.; Kanagawa, O.; Swanson, P. E.; Unanue, E. R. (1998): Chronic Listeria infection in SCID mice: requirements for the carrier state and the dual role of T cells in transferring protection or suppression. In *Journal of immunology (Baltimore, Md. : 1950)* 160 (1), pp. 376–384.

Bielecki, J.; Youngman, P.; Connelly, P.; Portnoy, D. A. (1990): Bacillus subtilis expressing a haemolysin gene from Listeria monocytogenes can grow in mammalian cells. In *Nature* 345 (6271), pp. 175–176. DOI: 10.1038/345175a0.

Blattman, Joseph N.; Wherry, E. John; Ha, Sang-Jun; van der Most, Robbert G.; Ahmed, Rafi (2009): Impact of epitope escape on PD-1 expression and CD8 T-cell exhaustion during chronic infection. In *Journal of virology* 83 (9), pp. 4386–4394. DOI: 10.1128/JVI.02524-08.

Boddupalli, Chandra Sekhar; Nair, Shiny; Gray, Simon M.; Nowyhed, Heba N.; Verma, Rakesh; Gibson, Joanna A. et al. (2016): ABC transporters and NR4A1 identify a quiescent subset of tissue-resident memory T cells. In *The Journal of clinical investigation* 126 (10), pp. 3905–3916. DOI: 10.1172/JCI85329.

Butz, Eric A.; Bevan, Michael J. (1998): Massive Expansion of Antigen-Specific CD8+ T Cells during an Acute Virus Infection. In *Immunity* 8 (2), pp. 167–175.

Carrero, Javier A.; Calderon, Boris; Unanue, Emil R. (2004): Type I interferon sensitizes lymphocytes to apoptosis and reduces resistance to Listeria infection. In *J Exp Med* 200 (4), pp. 535–540. DOI: 10.1084/jem.20040769.

Casey, Kerry A.; Fraser, Kathryn A.; Schenkel, Jason M.; Moran, Amy; Abt, Michael C.; Beura, Lalit K. et al. (2012): Antigen-independent differentiation and maintenance of effector-like resident memory T cells in tissues. In *J Immunol* 188 (10), pp. 4866–4875. DOI: 10.4049/jimmunol.1200402.

Cerf-Bensussan, N.; Jarry, A.; Brousse, N.; Lisowska-Grospierre, B.; Guy-Grand, D.; Griscelli, C. (1987): A monoclonal antibody (HML-1) defining a novel membrane molecule present on human intestinal lymphocytes. In *European journal of immunology* 17 (9), pp. 1279–1285. DOI: 10.1002/eji.1830170910.

Chakraborty, T.; Ebel, F.; Domann, E.; Niebuhr, K.; Gerstel, B.; Pistor, S. et al. (1995): A focal adhesion factor directly linking intracellularly motile Listeria monocytogenes and Listeria ivanovii to the actin-based cytoskeleton of mammalian cells. In *The EMBO Journal* 14 (7), pp. 1314–1321.

Chertov, O.; Yang, D.; Howard, O. M.; Oppenheim, J. J. (2000): Leukocyte granule proteins mobilize innate host defenses and adaptive immune responses. In *Immunological reviews* 177, pp. 68–78. DOI: 10.1034/j.1600-065X.2000.17702.x.

Cobleigh, Melissa A.; Bradfield, Clinton; Liu, Yuanjie; Mehta, Anand; Robek, Michael D. (2012): The immune response to a vesicular stomatitis virus vaccine vector is independent of particulate antigen secretion and protein turnover rate. In *Journal of virology* 86 (8), pp. 4253–4261. DOI: 10.1128/JVI.05991-11.

Cossart, P.; Vicente, M. F.; Mengaud, J.; Baquero, F.; Perez-Diaz, J. C.; Berche, P. (1989): Listeriolysin O is essential for virulence of Listeria monocytogenes: direct evidence obtained by gene complementation. In *Infection and Immunity* 57 (11), pp. 3629–3636.

Çuburu, Nicolas; Graham, Barney S.; Buck, Christopher B.; Kines, Rhonda C.; Pang, Yuk-Ying S.; Day, Patricia M. et al. (2012): Intravaginal immunization with HPV vectors induces tissue-resident CD8+ T cell responses. In *The Journal of clinical investigation* 122 (12), pp. 4606–4620. DOI: 10.1172/JCI63287.

Diaz, Leyla S.; Foster, Hillary; Stone, Mars R.; Fujimura, Sue; Relman, David A.; Levy, Jay A. (2005): VCAM-1 expression on CD8+ cells correlates with enhanced anti-HIV suppressing activity. In *Journal of immunology (Baltimore, Md. : 1950)* 174 (3), pp. 1574–1579. DOI: 10.4049/jimmunol.174.3.1574.

Diaz-Salazar, Carlos; Bou-Puerto, Regina; Mujal, Adriana M.; Lau, Colleen M.; Hoesslin, Madlaina von; Zehn, Dietmar; Sun, Joseph C. (2020): Cell-intrinsic adrenergic signaling controls the adaptive NK cell response to viral infection. In *The Journal of experimental medicine* 217 (4), e20190549. DOI: 10.1084/jem.20190549.

Dillon, S. R.; Jameson, S. C.; Fink, P. J. (1994): V beta 5+ T cell receptors skew toward OVA+H-2Kb recognition. In *Journal of immunology (Baltimore, Md. : 1950)* 152 (4), pp. 1790–1801.

Donocoff, Rachel S.; Teteloshvili, Nato; Chung, Hyunsoo; Shoulson, Rivka; Creusot, Remi J. (2020): Optimization of tamoxifen-induced Cre activity and its effect on immune cell populations. In *Scientific reports* 10 (1), p. 15244. DOI: 10.1038/s41598-020-72179-0.

Draper, R. K.; Simon, M. I. (1980): The entry of diphtheria toxin into the mammalian cell cytoplasm: evidence for lysosomal involvement. In *The Journal of cell biology* 87 (3 Pt 1), pp. 849–854. DOI: 10.1083/jcb.87.3.849.

Edelson, Brian T.; Bradstreet, Tara R.; Hildner, Kai; Carrero, Javier A.; Frederick, Katherine E.; KC, Wumesh et al. (2011): CD8α(+) dendritic cells are an obligate cellular entry point for productive infection by Listeria monocytogenes. In *Immunity* 35 (2), pp. 236–248. DOI: 10.1016/j.immuni.2011.06.012.

El-Asady, Riham; Yuan, Rongwen; Liu, Kechang; Wang, Donghua; Gress, Ronald E.; Lucas, Philip J. et al. (2005): TGF-{beta}-dependent CD103 expression by CD8(+) T cells promotes selective destruction of the host intestinal epithelium during graft-versus-host disease. In *J Exp Med* 201 (10), pp. 1647–1657. DOI: 10.1084/jem.20041044.

Feil, Susanne; Valtcheva, Nadejda; Feil, Robert (2009): Inducible Cre mice. In *Methods in molecular biology (Clifton, N.J.)* 530, pp. 343–363. DOI: 10.1007/978-1-59745-471-1_18.

Fernandez-Ruiz, Daniel; Ng, Wei Yi; Holz, Lauren E.; Ma, Joel Z.; Zaid, Ali; Wong, Yik Chun et al. (2016): Liver-Resident Memory CD8+ T Cells Form a Front-Line Defense against Malaria Liver-Stage Infection. In *Immunity* 45 (4), pp. 889–902. DOI: 10.1016/j.immuni.2016.08.011.

Flosbach, Markus; Oberle, Susanne G.; Scherer, Stefanie; Zecha, Jana; Hoesslin, Madlaina von; Wiede, Florian et al. (2020): PTPN2 Deficiency Enhances Programmed T Cell Expansion and Survival Capacity of Activated T Cells. In *Cell reports* 32 (4), p. 107957. DOI: 10.1016/j.celrep.2020.107957.

Gebhardt, Thomas; Wakim, Linda M.; Eidsmo, Liv; Reading, Patrick C.; Heath, William R.; Carbone, Francis R. (2009): Memory T cells in nonlymphoid tissue that provide enhanced local immunity during infection with herpes simplex virus. In *Nature immunology* 10 (5), pp. 524–530. DOI: 10.1038/ni.1718.

Gerlach, Carmen; Moseman, E. Ashley; Loughhead, Scott M.; Alvarez, David; Zwijnenburg, Anthonie J.; Waanders, Lisette et al. (2016): The Chemokine Receptor CX3CR1 Defines Three Antigen-Experienced CD8 T Cell Subsets with Distinct Roles in Immune Surveillance and Homeostasis. In *Immunity* 45 (6), pp. 1270–1284. DOI: 10.1016/j.immuni.2016.10.018.

Germain, Ronald N. (1994): MHC-dependent antigen processing and peptide presentation: Providing ligands for T lymphocyte activation. In *Cell* 76 (2), pp. 287–299. DOI: 10.1016/0092-8674(94)90336-0.

Guermonprez, Pierre; Valladeau, Jenny; Zitvogel, Laurence; Théry, Clotilde; Amigorena, Sebastian (2002): Antigen presentation and T cell stimulation by dendritic cells. In *Annual review of immunology* 20, pp. 621–667. DOI: 10.1146/annurev.immunol.20.100301.064828.

Guo, Jian-Kan; Shi, Hongmei; Koraishy, Farrukh; Marlier, Arnaud; Ding, Zhaowei; Shan, Alan; Cantley, Lloyd G. (2013): The Terminator mouse is a diphtheria toxin-receptor knock-in mouse strain for rapid and efficient enrichment of desired cell lineages. In *Kidney international* 84 (5), pp. 1041–1046. DOI: 10.1038/ki.2013.202.

Hadley, G. A.; Bartlett, S. T.; Via, C. S.; Rostapshova, E. A.; Moainie, S. (1997): The epithelial cell-specific integrin, CD103 (alpha E integrin), defines a novel subset of alloreactive CD8+ CTL. In *J Immunol* 159 (8), pp. 3748–3756.

Hansen, Scott G.; Ford, Julia C.; Lewis, Matthew S.; Ventura, Abigail B.; Hughes, Colette M.; Coyne-Johnson, Lia et al. (2011): Profound early control of highly pathogenic SIV by an effector memory T-cell vaccine. In *Nature* 473 (7348), pp. 523–527. DOI: 10.1038/nature10003.

Hardenberg, Jan-Hendrik B.; Braun, Andrea; Schon, Michael P. (2018): A Yin and Yang in Epithelial Immunology: The Roles of the alphaE(CD103)beta7 Integrin in T Cells. In *The Journal of investigative dermatology* 138 (1), pp. 23–31. DOI: 10.1016/j.jid.2017.05.026.

Haruyama, Naoto; Cho, Andrew; Kulkarni, Ashok B. (2009): Overview: engineering transgenic constructs and mice. In *Current protocols in cell biology* Chapter 19, Unit 19.10. DOI: 10.1002/0471143030.cb1910s42.

Heinzel, F. P.; Sadick, M. D.; Holaday, B. J.; Coffman, R. L.; Locksley, R. M. (1989): Reciprocal expression of interferon gamma or interleukin 4 during the resolution or progression of murine leishmaniasis. Evidence for expansion of distinct helper T cell subsets. In *J Exp Med* 169 (1), pp. 59–72. DOI: 10.1084/jem.169.1.59.

Hogquist, Kristin A.; Jameson, Stephen C.; Heath, William R.; Howard, Jane L.; Bevan, Michael J.; Carbone, Francis R. (1994): T cell receptor antagonist peptides induce positive selection. In *Cell* 76 (1), pp. 17–27. DOI: 10.1016/0092-8674(94)90169-4.

Im, Se Jin; Konieczny, Bogumila T.; Hudson, William H.; Masopust, David; Ahmed, Rafi (2020): PD-1+ stemlike CD8 T cells are resident in lymphoid tissues during persistent LCMV infection. In *Proceedings of the National Academy of Sciences of the United States of America* 117 (8), pp. 4292–4299. DOI: 10.1073/pnas.1917298117.

Jiang, Xiaodong; Clark, Rachael A.; Liu, Luzheng; Wagers, Amy J.; Fuhlbrigge, Robert C.; Kupper, Thomas S. (2012): Skin infection generates non-migratory memory CD8+ T(RM) cells providing global skin immunity. In *Nature* 483 (7388), pp. 227–231. DOI: 10.1038/nature10851.

Kadoki, Motohiko; Patil, Ashwini; Thaiss, Cornelius C.; Brooks, Donald J.; Pandey, Surya; Deep, Deeksha et al. (2017): Organism-Level Analysis of Vaccination Reveals Networks of Protection across Tissues. In *Cell* 171 (2), 398-413.e21. DOI: 10.1016/j.cell.2017.08.024.

Kaech, Susan M.; Tan, Joyce T.; Wherry, E. John; Konieczny, Bogumila T.; Surh, Charles D.; Ahmed, Rafi (2003): Selective expression of the interleukin 7 receptor identifies effector CD8 T cells that give rise to long-lived memory cells. In *Nat Immunol* 4 (12), pp. 1191–1198. DOI: 10.1038/ni1009.

Kilshaw, P. J.; Murant, S. J. (1990): A new surface antigen on intraepithelial lymphocytes in the intestine. In *European journal of immunology* 20 (10), pp. 2201–2207. DOI: 10.1002/eji.1830201008.

Kim, Jeong M.; Rasmussen, Jeffrey P.; Rudensky, Alexander Y. (2007): Regulatory T cells prevent catastrophic autoimmunity throughout the lifespan of mice. In *Nat Immunol* 8 (2), pp. 191–197. DOI: 10.1038/ni1428.

Kim, S. K.; Reed, D. S.; Olson, S.; Schnell, M. J.; Rose, J. K.; Morton, P. A.; Lefrançois, L. (1998): Generation of mucosal cytotoxic T cells against soluble protein by tissue-specific environmental and costimulatory signals. In *Proceedings of the National Academy of Sciences of the United States of America* 95 (18), pp. 10814–10819. DOI: 10.1073/pnas.95.18.10814.

Kocks, C.; Gouin, E.; Tabouret, M.; Berche, P.; Ohayon, H.; Cossart, P. (1992): L. monocytogenes-induced actin assembly requires the actA gene product, a surface protein. In *Cell* 68 (3), pp. 521–531. DOI: 10.1016/0092-8674(92)90188-i.

Kurachi, Makoto; Ngiow, Shin Foong; Kurachi, Junko; Chen, Zeyu; Wherry, E. John (2019): Hidden Caveat of Inducible Cre Recombinase. In *Immunity* 51 (4), pp. 591–592. DOI: 10.1016/j.immuni.2019.09.010.

Kurd, Nadia S.; He, Zhaoren; Louis, Tiani L.; Milner, J. Justin; Omilusik, Kyla D.; Jin, Wenhao et al. (2020): Early precursors and molecular determinants of tissue-resident memory CD8+ T lymphocytes revealed by single-cell RNA sequencing. In *Science immunology* 5 (47). DOI: 10.1126/sciimmunol.aaz6894.

Larsson, B. M.; Larsson, K.; Malmberg, P.; Palmberg, L. (1999): Gram positive bacteria induce IL-6 and IL-8 production in human alveolar macrophages and epithelial cells. In *Inflammation* 23 (3), pp. 217–230. DOI: 10.1023/a:1020269802315.

Le Floc'h, Audrey; Jalil, Abdelali; Vergnon, Isabelle; Le Maux Chansac, Beatrice; Lazar, Vladimir; Bismuth, Georges et al. (2007): Alpha E beta 7 integrin interaction with E-cadherin promotes antitumor CTL activity by triggering lytic granule polarization and exocytosis. In *J Exp Med* 204 (3), pp. 559–570. DOI: 10.1084/jem.20061524.

Lee, K. J.; Novella, I. S.; Teng, M. N.; Oldstone, M. B.; La Torre, J. C. de (2000): NP and L proteins of lymphocytic choriomeningitis virus (LCMV) are sufficient for efficient transcription and replication of LCMV genomic RNA analogs. In *Journal of virology* 74 (8), pp. 3470–3477. DOI: 10.1128/jvi.74.8.3470-3477.2000.

Lewis, Steven M.; Williams, Adam; Eisenbarth, Stephanie C. (2019): Structure and function of the immune system in the spleen. In *Science immunology* 4 (33). DOI: 10.1126/sciimmunol.aau6085.

Lichty, Brian D.; Power, Anthony T.; Stojdl, David F.; Bell, John C. (2004): Vesicular stomatitis virus: re-inventing the bullet. In *Trends in molecular medicine* 10 (5), pp. 210–216. DOI: 10.1016/j.molmed.2004.03.003.

López-Cabrera, M.; Muñoz, E.; Blázquez, M. V.; Ursa, M. A.; Santis, A. G.; Sánchez-Madrid, F. (1995): Transcriptional regulation of the gene encoding the human C-type lectin leukocyte receptor AIM/CD69 and functional characterization of its tumor necrosis factor-alpha-responsive elements. In *The Journal of biological chemistry* 270 (37), pp. 21545–21551. DOI: 10.1074/jbc.270.37.21545.

Mackay, Laura K.; Minnich, Martina; Kragten, Natasja A. M.; Liao, Yang; Nota, Benjamin; Seillet, Cyril et al. (2016): Hobit and Blimp1 instruct a universal transcriptional program of tissue residency in lymphocytes. In *Science (New York, N.Y.)* 352 (6284), pp. 459–463. DOI: 10.1126/science.aad2035.

Mackay, Laura K.; Rahimpour, Azad; Ma, Joel Z.; Collins, Nicholas; Stock, Angus T.; Hafon, Ming-Li et al. (2013a): The developmental pathway for CD103+CD8+ tissue-resident memory T cells of skin. In *Nat Immunol* 14 (12), pp. 1294–1301. DOI: 10.1038/ni.2744.

Mackay, Laura K.; Rahimpour, Azad; Ma, Joel Z.; Collins, Nicholas; Stock, Angus T.; Hafon, Ming-Li et al. (2013b): The developmental pathway for CD103+CD8+ tissue-resident memory T cells of skin. In *Nat Immunol* 14 (12), pp. 1294–1301. DOI: 10.1038/ni.2744.

Mackay, Laura K.; Stock, Angus T.; Ma, Joel Z.; Jones, Claerwen M.; Kent, Stephen J.; Mueller, Scott N. et al. (2012): Long-lived epithelial immunity by tissue-resident memory T (TRM) cells in the absence of persisting local antigen presentation. In *Proceedings of the National Academy of Sciences of the United States of America* 109 (18), pp. 7037–7042. DOI: 10.1073/pnas.1202288109.

Martinez, Isidoro; Wertz, Gail W. (2005): Biological differences between vesicular stomatitis virus Indiana and New Jersey serotype glycoproteins: identification of amino acid residues modulating pH-dependent infectivity. In *Journal of virology* 79 (6), pp. 3578–3585. DOI: 10.1128/JVI.79.6.3578-3585.2005.

Masopust, David; Choo, Daniel; Vezys, Vaiva; Wherry, E. John; Duraiswamy, Jaikumar; Akondy, Rama et al. (2010): Dynamic T cell migration program provides

resident memory within intestinal epithelium. In *J Exp Med* 207 (3), pp. 553–564. DOI: 10.1084/jem.20090858.

Masopust, David; Soerens, Andrew G. (2019): Tissue-Resident T Cells and Other Resident Leukocytes. In *Annual review of immunology* 37, pp. 521–546. DOI: 10.1146/annurev-immunol-042617-053214.

Masopust, David; Vezys, Vaiva; Usherwood, Edward J.; Cauley, Linda S.; Olson, Sara; Marzo, Amanda L. et al. (2004): Activated primary and memory CD8 T cells migrate to nonlymphoid tissues regardless of site of activation or tissue of origin. In *J Immunol* 172 (8), pp. 4875–4882. DOI: 10.4049/jimmunol.172.8.4875.

Masopust, David; Vezys, Vaiva; Wherry, E. John; Barber, Daniel L.; Ahmed, Rafi (2006): Cutting edge: gut microenvironment promotes differentiation of a unique memory CD8 T cell population. In *J Immunol* 176 (4), pp. 2079–2083. DOI: 10.4049/jimmunol.176.4.2079.

Matloubian, M.; Kolhekar, S. R.; Somasundaram, T.; Ahmed, R. (1993): Molecular determinants of macrophage tropism and viral persistence: importance of single amino acid changes in the polymerase and glycoprotein of lymphocytic choriomeningitis virus. In *Journal of virology* 67 (12), pp. 7340–7349. DOI: 10.1128/JVI.67.12.7340-7349.1993.

McMaster, Sean R.; Wilson, Jarad J.; Wang, Hong; Kohlmeier, Jacob E. (2015): Airway-Resident Memory CD8 T Cells Provide Antigen-Specific Protection against Respiratory Virus Challenge through Rapid IFN-γ Production. In *Journal of immunology (Baltimore, Md. : 1950)* 195 (1), pp. 203–209. DOI: 10.4049/jimmunol.1402975.

McQuin, Claire; Goodman, Allen; Chernyshev, Vasiliy; Kamentsky, Lee; Cimini, Beth A.; Karhohs, Kyle W. et al. (2018): CellProfiler 3.0: Next-generation image processing for biology. In *PLoS biology* 16 (7), e2005970. DOI: 10.1371/journal.pbio.2005970.

Meunier, Sylvain; Rapetti, Laëtitia; Beziaud, Laurent; Pontoux, Christiane; Legrand, Agnès; Tanchot, Corinne (2012): Synergistic CD40 signaling on APCs and CD8 T cells drives efficient CD8 response and memory differentiation. In *Journal of leukocyte biology* 91 (6), pp. 859–869. DOI: 10.1189/jlb.0611292.

Meyer, Michelle; Garron, Tania; Lubaki, Ndongala M.; Mire, Chad E.; Fenton, Karla A.; Klages, Curtis et al. (2015): Aerosolized Ebola vaccine protects primates and elicits lung-resident T cell responses. In *The Journal of clinical investigation* 125 (8), pp. 3241–3255. DOI: 10.1172/JCI81532.

Miller, J. F.; Mitchell, G. F. (1968): Cell to cell interaction in the immune response. I. Hemolysin-forming cells in neonatally thymectomized mice reconstituted with thymus or thoracic duct lymphocytes. In *J Exp Med* 128 (4), pp. 801–820. DOI: 10.1084/jem.128.4.801.

Milner, J. Justin; Toma, Clara; He, Zhaoren; Kurd, Nadia S.; Nguyen, Quynh P.; McDonald, Bryan et al. (2020): Heterogenous Populations of Tissue-Resident CD8+ T Cells Are Generated in Response to Infection and Malignancy. In *Immunity* 52 (5), 808-824.e7. DOI: 10.1016/j.immuni.2020.04.007.

Milner, J. Justin; Toma, Clara; Yu, Bingfei; Zhang, Kai; Omilusik, Kyla; Phan, Anthony T. et al. (2017): Runx3 programs CD8+ T cell residency in non-lymphoid tissues and tumours. In *Nature* 552 (7684), pp. 253–257. DOI: 10.1038/nature24993.

Mitamura, T.; Higashiyama, S.; Taniguchi, N.; Klagsbrun, M.; Mekada, E. (1995): Diphtheria toxin binds to the epidermal growth factor (EGF)-like domain of human heparin-binding EGF-like growth factor/diphtheria toxin receptor and inhibits specifically its mitogenic activity. In *The Journal of biological chemistry* 270 (3), pp. 1015–1019. DOI: 10.1074/jbc.270.3.1015.

Moyat, M.; Bouzourene, H.; Ouyang, W.; Iovanna, J.; Renauld, J-C; Velin, D. (2017): IL-22-induced antimicrobial peptides are key determinants of mucosal vaccine-induced protection against H. pylori in mice. In *Mucosal immunology* 10 (1), pp. 271–281. DOI: 10.1038/mi.2016.38.

Naglich, Joseph G.; Metherall, James E.; Russell, David W.; Eidels, Leon (1992): Expression cloning of a diphtheria toxin receptor: Identity with a heparin-binding EGF-like growth factor precursor. In *Cell* 69 (6), pp. 1051–1061. DOI: 10.1016/0092-8674(92)90623-K.

Nizard, Mevyn; Roussel, Hélène; Diniz, Mariana O.; Karaki, Soumaya; Tran, Thi; Voron, Thibault et al. (2017): Induction of resident memory T cells enhances the efficacy of cancer vaccine. In *Nature communications* 8, p. 15221. DOI: 10.1038/ncomms15221.

Oberle, Susanne G.; Hanna-El-Daher, Layane; Chennupati, Vijaykumar; Enouz, Sarah; Scherer, Stefanie; Prlic, Martin; Zehn, Dietmar (2016): A Minimum Epitope Overlap between Infections Strongly Narrows the Emerging T Cell Repertoire. In *Cell reports* 17 (3), pp. 627–635. DOI: 10.1016/j.celrep.2016.09.072.

Omilusik, Kyla; Milner, J. Justin; Kurd, Nadia; Toma, Clara; Chang, John T.; Goldrath, Ananda W. (2019): Identification of TRM subsets with distinct cellular states and memory potential. In *J Immunol* 202 (1), Supplement. Available online at https://www.jimmunol.org/content/202/1_Supplement/60.14, checked on 1/13/2019.

Osborn, Jossef F.; Mooster, Jana L.; Hobbs, Samuel J.; Munks, Michael W.; Barry, Conrad; Harty, John T. et al. (2017): Enzymatic synthesis of core 2 O-glycans governs the tissue-trafficking potential of memory CD8+ T cells. In *Science immunology* 2 (16). DOI: 10.1126/sciimmunol.aan6049.

Oxenius, Annette; Bachmann, Martin F.; Zinkernagel, Rolf M.; Hengartner, Hans (1998): Virus-specific major MHC class II-restricted TCR-transgenic mice: effects on humoral and cellular immune responses after viral infection. In *Eur. J. Immunol.* 28 (1), pp. 390–400. DOI: 10.1002/(SICI)1521-4141(199801)28:01<390::AID-IMMU390>3.0.CO;2-O.

Pamer, Eric G. (2004): Immune responses to Listeria monocytogenes. In *Nature reviews. Immunology* 4 (10), pp. 812–823. DOI: 10.1038/nri1461.

Pappenheimer, A. M.; Harper, A. A.; Moynihan, M.; Brockes, J. P. (1982): Diphtheria toxin and related proteins: effect of route of injection on toxicity and the determination of cytotoxicity for various cultured cells. In *The Journal of infectious diseases* 145 (1), pp. 94–102. DOI: 10.1093/infdis/145.1.94.

Park, Simone L.; Zaid, Ali; Hor, Jyh Liang; Christo, Susan N.; Prier, Julia E.; Davies, Brooke et al. (2018): Local proliferation maintains a stable pool of tissue-resident memory T cells after antiviral recall responses. In *Nature immunology* 19 (2), pp. 183–191. DOI: 10.1038/s41590-017-0027-5.

Perez, Oriana A.; Yeung, Stephen T.; Vera-Licona, Paola; Romagnoli, Pablo A.; Samji, Tasleem; Ural, Basak B. et al. (2017): CD169+ macrophages orchestrate innate immune responses by regulating bacterial localization in the spleen. In *Science immunology* 2 (16). DOI: 10.1126/sciimmunol.aah5520.

Pircher, H.; Moskophidis, D.; Rohrer, U.; Bürki, K.; Hengartner, H.; Zinkernagel, R. M. (1990): Viral escape by selection of cytotoxic T cell-resistant virus variants in vivo. In *Nature* 346 (6285), pp. 629–633. DOI: 10.1038/346629a0.

Puglielli, M. T.; Zajac, A. J.; van der Most, R. G.; Dzuris, J. L.; Sette, A.; Altman, J. D.; Ahmed, R. (2001): In vivo selection of a lymphocytic choriomeningitis virus variant that affects recognition of the GP33-43 epitope by H-2Db but not H-2Kb. In *Journal of virology* 75 (11), pp. 5099–5107. DOI: 10.1128/JVI.75.11.5099-5107.2001.

Richer, Martin J.; Nolz, Jeffrey C.; Harty, John T. (2013): Pathogen-specific inflammatory milieux tune the antigen sensitivity of CD8(+) T cells by enhancing T cell receptor signaling. In *Immunity* 38 (1), pp. 140–152. DOI: 10.1016/j.immuni.2012.09.017.

Saito, M.; Iwawaki, T.; Taya, C.; Yonekawa, H.; Noda, M.; Inui, Y. et al. (2001): Diphtheria toxin receptor-mediated conditional and targeted cell ablation in transgenic mice. In *Nature biotechnology* 19 (8), pp. 746–750. DOI: 10.1038/90795.

Sallusto, Frederica; Danielle Lenig; Reinhold Förster; Martin Lipp; Antonio Lanzavecchia (1999): Two subsets of memory T lymphocytes with distinct homing potentials and effector functions. In *Nature* 401 (6754), pp. 708–712. DOI: 10.1038/44385.

Salvato, Maria; Shimomaye, Elaine; Southern, Peter; Oldstone, Michael B.A. (1988): Virus-lymphocyte interactions IV. Molecular characterization of LCMV Armstrong (CTL+) small genomic segment and that of its variant, clone 13 (CTL−). In *Virology* 164 (2), pp. 517–522. DOI: 10.1016/0042-6822(88)90566-1.

Sandvig, K.; Olsnes, S. (1980): Diphtheria toxin entry into cells is facilitated by low pH. In *The Journal of cell biology* 87 (3 Pt 1), pp. 828–832. DOI: 10.1083/jcb.87.3.828.

Sauer, B.; Henderson, N. (1988): Site-specific DNA recombination in mammalian cells by the Cre recombinase of bacteriophage P1. In *Proceedings of the National Academy of Sciences of the United States of America* 85 (14), pp. 5166–5170. DOI: 10.1073/pnas.85.14.5166.

Schenkel, Jason M.; Fraser, Kathryn A.; Beura, Lalit K.; Pauken, Kristen E.; Vezys, Vaiva; Masopust, David (2014a): T cell memory. Resident memory CD8 T cells trigger protective innate and adaptive immune responses. In *Science (New York, N.Y.)* 346 (6205), pp. 98–101. DOI: 10.1126/science.1254536.

Schenkel, Jason M.; Fraser, Kathryn A.; Masopust, David (2014b): Cutting edge: resident memory CD8 T cells occupy frontline niches in secondary lymphoid organs. In *The Journal of Immunology* 192 (7), pp. 2961–2964. DOI: 10.4049/jimmunol.1400003.

Schenkel, Jason M.; Fraser, Kathryn A.; Vezys, Vaiva; Masopust, David (2013): Sensing and alarm function of resident memory $CD8^+$ T cells. In *Nature immunology* 14 (5), pp. 509–513. DOI: 10.1038/ni.2568.

Schneider, Marlon R.; Wolf, Eckhard (2009): The epidermal growth factor receptor ligands at a glance. In *Journal of cellular physiology* 218 (3), pp. 460–466. DOI: 10.1002/jcp.21635.

Seidman, J. G.; Leder, P. (1978): The arrangement and rearrangement of antibody genes. In *Nature* 276 (5690), pp. 790–795. DOI: 10.1038/276790a0.

Serbina, Natalya V.; Shi, Chao; Pamer, Eric G. (2012): Monocyte-mediated immune defense against murine Listeria monocytogenes infection. In *Advances in immunology* 113, pp. 119–134. DOI: 10.1016/B978-0-12-394590-7.00003-8.

Shimshek, D. R.; Kim, J.; Hübner, M. R.; Spergel, D. J.; Buchholz, F.; Casanova, E. et al. (2002): Codon-improved Cre recombinase (iCre) expression in the mouse. In *Genesis (New York, N.Y. : 2000)* 32 (1), pp. 19–26. DOI: 10.1002/gene.10023.

Siddiqui, Sarah; Basta, Sameh (2011): CD8+ T cell immunodominance in lymphocytic choriomeningitis virus infection is modified in the presence of toll-like receptor agonists. In *Journal of virology* 85 (24), pp. 13224–13233. DOI: 10.1128/JVI.05996-11.

Simms, P. E.; Ellis, T. M. (1996): Utility of flow cytometric detection of CD69 expression as a rapid method for determining poly- and oligoclonal lymphocyte activation. In *Clinical and Diagnostic Laboratory Immunology* 3 (3), pp. 301–304.

Skon, Cara N.; Lee, June-Yong; Anderson, Kristin G.; Masopust, David; Hogquist, Kristin A.; Jameson, Stephen C. (2013): Transcriptional downregulation of S1pr1

is required for the establishment of resident memory CD8+ T cells. In *Nat Immunol* 14 (12), pp. 1285–1293. DOI: 10.1038/ni.2745.

Smith, Logan K.; Boukhaled, Giselle M.; Condotta, Stephanie A.; Mazouz, Sabrina; Guthmiller, Jenna J.; Vijay, Rahul et al. (2018): Interleukin-10 Directly Inhibits CD8+ T Cell Function by Enhancing N-Glycan Branching to Decrease Antigen Sensitivity. In *Immunity* 48 (2), 299-312.e5. DOI: 10.1016/j.immuni.2018.01.006.

Smyth, L. J. C.; Kirby, J. A.; Cunningham, A. C. (2007): Role of the mucosal integrin alpha(E)(CD103)beta(7) in tissue-restricted cytotoxicity. In *Clinical and experimental immunology* 149 (1), pp. 162–170. DOI: 10.1111/j.1365-2249.2007.03385.x.

Soudja, Saïdi M'Homa; Ruiz, Anne L.; Marie, Julien C.; Lauvau, Grégoire (2012): Inflammatory monocytes activate memory CD8(+) T and innate NK lymphocytes independent of cognate antigen during microbial pathogen invasion. In *Immunity* 37 (3), pp. 549–562. DOI: 10.1016/j.immuni.2012.05.029.

Steinbach, Karin; Vincenti, Ilena; Kreutzfeldt, Mario; Page, Nicolas; Muschaweckh, Andreas; Wagner, Ingrid et al. (2016): Brain-resident memory T cells represent an autonomous cytotoxic barrier to viral infection. In *J Exp Med* 213 (8), pp. 1571–1587. DOI: 10.1084/jem.20151916.

Steinert, Elizabeth M.; Schenkel, Jason M.; Fraser, Kathryn A.; Beura, Lalit K.; Manlove, Luke S.; Igyártó, Botond Z. et al. (2015): Quantifying Memory CD8 T Cells Reveals Regionalization of Immunosurveillance. In *Cell* 161 (4), pp. 737–749. DOI: 10.1016/j.cell.2015.03.031.

Stringer, Carsen; Wang, Tim; Michaelos, Michalis; Pachitariu, Marius (2020): Cellpose: a generalist algorithm for cellular segmentation. In *Nature methods*. DOI: 10.1109/TPAMI.2006.253.

Szabo, Peter A.; Miron, Michelle; Farber, Donna L. (2019): Location, location, location: Tissue resident memory T cells in mice and humans. In *Science immunology* 4 (34). DOI: 10.1126/sciimmunol.aas9673.

Tsuneoka, M.; Nakayama, K.; Hatsuzawa, K.; Komada, M.; Kitamura, N.; Mekada, E. (1993): Evidence for involvement of furin in cleavage and activation of diphtheria toxin. In *The Journal of biological chemistry* 268 (35), pp. 26461–26465.

Turner, Damian L.; Cauley, Linda S.; Khanna, Kamal M.; Lefrançois, Leo (2007): Persistent antigen presentation after acute vesicular stomatitis virus infection. In *Journal of virology* 81 (4), pp. 2039–2046. DOI: 10.1128/JVI.02167-06.

Waite, Janelle C.; Leiner, Ingrid; Lauer, Peter; Rae, Chris S.; Barbet, Gaetan; Zheng, Huan et al. (2011): Dynamic imaging of the effector immune response to listeria infection in vivo. In *PLoS pathogens* 7 (3), e1001326. DOI: 10.1371/journal.ppat.1001326.

Walsh, Daniel A.; Borges da Silva, Henrique; Beura, Lalit K.; Peng, Changwei; Hamilton, Sara E.; Masopust, David; Jameson, Stephen C. (2019): The Functional Requirement for CD69 in Establishment of Resident Memory CD8+ T Cells Varies with Tissue Location. In *Journal of immunology (Baltimore, Md. : 1950)* 203 (4), pp. 946–955. DOI: 10.4049/jimmunol.1900052.

Wang, Bo; Wu, Shaoxu; Zeng, Hong; Liu, Zhuowei; Dong, Wen; He, Wang et al. (2015): CD103+ Tumor Infiltrating Lymphocytes Predict a Favorable Prognosis in Urothelial Cell Carcinoma of the Bladder. In *The Journal of urology* 194 (2), pp. 556–562. DOI: 10.1016/j.juro.2015.02.2941.

Webb, John R.; Milne, Katy; Nelson, Brad H. (2015): PD-1 and CD103 Are Widely Coexpressed on Prognostically Favorable Intraepithelial CD8 T Cells in Human Ovarian Cancer. In *Cancer immunology research* 3 (8), pp. 926–935. DOI: 10.1158/2326-6066.CIR-14-0239.

Whitfield, Jonathan; Littlewood, Trevor; Soucek, Laura (2015): Tamoxifen administration to mice. In *Cold Spring Harbor protocols* 2015 (3), pp. 269–271. DOI: 10.1101/pdb.prot077966.

Witter, Alexandra R.; Okunnu, Busola M.; Berg, Rance E. (2016): The Essential Role of Neutrophils during Infection with the Intracellular Bacterial Pathogen Listeria monocytogenes. In *Journal of immunology (Baltimore, Md. : 1950)* 197 (5), pp. 1557–1565. DOI: 10.4049/jimmunol.1600599.

Wollert, Thomas; Pasche, Bastian; Rochon, Maike; Deppenmeier, Stefanie; van den Heuvel, Joop; Gruber, Achim D. et al. (2007): Extending the host range of Listeria monocytogenes by rational protein design. In *Cell* 129 (5), pp. 891–902. DOI: 10.1016/j.cell.2007.03.049.

Zehn, Dietmar; Lee, Sarah Y.; Bevan, Michael J. (2009): Complete but curtailed T-cell response to very low-affinity antigen. In *Nature* 458 (7235), pp. 211–214. DOI: 10.1038/nature07657.

Zhang, Nu; Bevan, Michael J. (2013): Transforming growth factor-beta signaling controls the formation and maintenance of gut-resident memory T cells by regulating migration and retention. In *Immunity* 39 (4), pp. 687–696. DOI: 10.1016/j.immuni.2013.08.019.

Zhou, Angela C.; Batista, Nathália V.; Watts, Tania H. (2019): 4-1BB Regulates Effector CD8 T Cell Accumulation in the Lung Tissue through a TRAF1-, mTOR-, and Antigen-Dependent Mechanism to Enhance Tissue-Resident Memory T Cell Formation during Respiratory Influenza Infection. In *The Journal of Immunology* 202 (8), pp. 2482–2492. DOI: 10.4049/jimmunol.1800795.

Zhou, Xin; Ramachandran, Srividya; Mann, Margaret; Popkin, Daniel L. (2012): Role of lymphocytic choriomeningitis virus (LCMV) in understanding viral immunology: past, present and future. In *Viruses* 4 (11), pp. 2650–2669. DOI: 10.3390/v4112650.

Zinkernagel, R. M.; Doherty, P. C. (1974a): Immunological surveillance against altered self components by sensitised T lymphocytes in lymphocytic choriomeningitis. In *Nature* 251 (5475), pp. 547–548. DOI: 10.1038/251547a0.

Zinkernagel, R. M.; Doherty, P. C. (1974b): Restriction of in vitro T cell-mediated cytotoxicity in lymphocytic choriomeningitis within a syngeneic or semiallogeneic system. In *Nature* 248 (5450), pp. 701–702. DOI: 10.1038/248701a0.

Acknowledgement

Finally, I would like to express my gratitude to all the people that supported me during the process.

I would like to thank my supervisor Prof. Dr. Dietmar Zehn for giving me the opportunity to do my PhD thesis in his group. Thank you for the chance to learn from a great role model for scientific thinking and personal determination. I am grateful for the freedom and unlimited support to develop myself on a scientific and a personal level.

I want to thank Dr. Bastian Höchst, who encouraged me to start the PhD and supported me throughout the process in scientific and personal matters.

I also want to thank all the people in the lab, who took time to help me and provided technical support. I am grateful, that I could work in a scientifically stimulating and deeply supportive environment especially thanks to Dr. Francesca Alfei, Dr. Stefanie Scherer, Jacqueline Berner, Miriam Kuhlman and Ann-Katrin Gerullis.

I thank my family and especially Sandra and Anina von Hösslin who were always there when I needed emotional support and who believed in me, when I was struggling.

Finally, I want to thank my husband and best friend Dr. Stefan von Hößlin. I am grateful that we always make it our aim to grow personally and professionally, and that we thus continually create exciting life tasks for ourselves. Thank you for your curiosity and deep interest in my goals, which gives me self-confidence in challenging times.